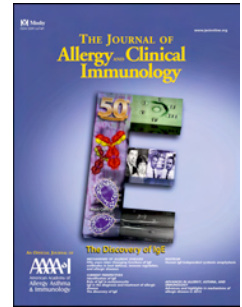


Accepted Manuscript

New mechanism underlying IL-31-induced atopic dermatitis

Jianghui Meng, PhD, Masaki Moriyama, PhD, Micha Feld, PhD, Joerg Buddenkotte, MD PhD, Timo Buhl, MD, Attila Szöllösi, PhD, Jingming Zhang, PhD, Paul Miller, PhD, Andre Ghetti, PhD, Michael Fischer, MD, Peter W. Reeh, MD, Chunxu Shan, PhD, Jiafu Wang, PhD, Martin Steinhoff, MD PhD



PII: S0091-6749(18)30214-8

DOI: [10.1016/j.jaci.2017.12.1002](https://doi.org/10.1016/j.jaci.2017.12.1002)

Reference: YMAI 13283

To appear in: *Journal of Allergy and Clinical Immunology*

Received Date: 12 June 2017

Revised Date: 18 November 2017

Accepted Date: 21 December 2017

Please cite this article as: Meng J, Moriyama M, Feld M, Buddenkotte J, Buhl T, Szöllösi A, Zhang J, Miller P, Ghetti A, Fischer M, Reeh PW, Shan C, Wang J, Steinhoff M, New mechanism underlying IL-31-induced atopic dermatitis, *Journal of Allergy and Clinical Immunology* (2018), doi: 10.1016/j.jaci.2017.12.1002.

This is a PDF file of an unedited manuscript that has been accepted for publication. As a service to our customers we are providing this early version of the manuscript. The manuscript will undergo copyediting, typesetting, and review of the resulting proof before it is published in its final form. Please note that during the production process errors may be discovered which could affect the content, and all legal disclaimers that apply to the journal pertain.

1 New mechanism underlying IL-31-induced atopic dermatitis

2

3 Jianghui Meng PhD^{1, 2*}, Masaki Moriyama PhD³, Micha Feld PhD⁴, Joerg Buddenkotte
4 MD PhD^{5,6}, Timo Buhl MD⁷, Attila Szöllösi PhD², Jingming Zhang PhD⁸, Paul Miller
5 PhD⁸, Andre Ghetti PhD⁸, Michael Fischer MD⁹, Peter W. Reeh MD¹⁰, Chunxu Shan
6 PhD^{1,2}, Jiafu Wang PhD¹, and Martin Steinhoff MD PhD^{2,3,5,6*}

7

- 8 1. International Center for Neurotherapeutics, Dublin City University, Dublin, Ireland.
- 9 2. Department of Dermatology and UCD Charles Institute for Translational
10 Dermatology, Dublin 4, Ireland.
- 11 3. Dept. of Dermatology, University of California, San Francisco, CA, U.S.A. Current
12 affiliation; Pharmaceutical Research Laboratories, Toray Industries, Inc., Kanagawa,
13 Japan.
- 14 4. Department of Dermatology, University Hospital Düsseldorf, Düsseldorf, Germany.
- 15 5. Department of Dermatology and Venereology, Hamad Medical Corporation, Qatar
16 University, Doha, Qatar.
- 17 6. School of Medicine, Weill Cornell University-Qatar and Qatar University, Doha,
18 Qatar.
- 19 7. Department of Dermatology, University Medical Center Göttingen, Göttingen,
20 Germany.
- 21 8. AnaBios Corporation, San Diego, CA U.S.A
- 22 9. Center for Physiology and Pharmacology, Medical University of Vienna, Vienna,
23 Austria.
- 24 10. Institut für Physiologie & Pathophysiologie, Universität Erlangen-Nürnberg,
25 Universitätsstraße 17, 91054 Erlangen, Germany.

26

27

28 *Corresponding Authors:

29 Dr Jianghui Meng (jianghui.meng@dcu.ie) and

30 Prof. Martin Steinhoff (martin.steinhoff@ucd.ie)

31 Phone: +353-1-700-7361 (JM) or +353-1-716-6269 (MS)

32

33 Declaration of all sources of funding

34 Science Foundation Ireland is thanked for funding this research through a Starting
35 Investigator Award (to J.M. Grant Number 15/SIRG/3508T), a Principle Investigator
36 Award (to M.S.) and a Career Development Award (13/CDA/2093 to JW). M.S. received
37 Excellence seed funding from Hamad Medical Corporation, Qatar.

38

39 **ABSTRACT**

40 **BACKGROUND:** T helper type 2 cell-released interleukin 31 (IL-31) is a critical mediator
41 in atopic dermatitis (AD), a prevalent and debilitating chronic skin disorder. Brain-derived
42 natriuretic peptide (BNP) has been described as a central itch mediator. The importance of
43 BNP in peripheral (skin-derived) itch and its functional link to IL-31 within the neuro-
44 immune axis of the skin is unknown.

45 **OBJECTIVE:** To investigate the function of BNP in the peripheral sensory system and
46 skin in IL-31-induced itch and neuro-epidermal communication in AD.

47 **METHODS:** Ca²⁺-imaging, immunohistochemistry, quantitative real-time PCR, RNA-Seq,
48 knockdown, cytokine/phosphor-kinase arrays, enzyme immune assay and pharmacological
49 inhibition were subjected to examine the cellular basis of the IL-31-stimulated, BNP-
50 related itch signaling in human DRG neurons (hDRG) and skin cells, transgenic AD-like
51 mouse models, and human skin of AD and healthy subjects.

52 **RESULTS:** In hDRG, we confirmed expression and co-occurrence of OSMR β and IL-31
53 receptor A in a small subset of neuronal population. Furthermore, IL-31 activated ~50% of
54 endothelin-1-responsive neurons, and half of the latter also responded to histamine. In
55 murine DRGs IL-31 upregulated *Nppb* and induced SNARE-dependent BNP release. In the
56 *Grhl3PAR2*^{+/+} mice, house dust mite-induced severe AD-like dermatitis was associated with
57 *Nppb* upregulation. Lesional IL-31Tg mice also exhibited increased *Nppb* transcripts in
58 DRGs and skin; accordingly, skin BNP receptor was elevated. Importantly, expression of
59 BNP and its receptor were increased in AD patient skin. In human skin cells, BNP
60 stimulated a pro-inflammatory, itch-promoting phenotype.

61 **CONCLUSION:** Our findings show, for the first time, that BNP is implicated in AD and
62 that IL-31 regulates BNP in both DRGs and skin. IL-31 enhances BNP release and
63 synthesis, and orchestrates cytokine and chemokine release from skin cells, thereby
64 coordinating the signaling pathways involved in itch. Inhibiting peripheral BNP function
65 may be a novel therapeutic strategy for AD and pruritic conditions.

66

67

68 KEY MESSAGES

69

- 70 • IL-31 induces SNARE-dependent BNP release and its synthesis in sensory nerves.
71 • BNP increases AD-related cytokine release from keratinocytes and dendritic cells
72 through GSK3-dependent and C-Jun activation pathways, respectively.
73 • AD is associated with upregulation of BNP and its receptor.

74

75

76 CAPSULE SUMMARY

77

78 Our study provides a novel functional link between IL-31 and BNP within the neuro-
79 immune axis of AD. Blockade of BNP release by inactivating SNAREs offers new strategy
80 for management of AD and pruritic conditions.

81

82

83

84 KEY WORDS

85

86 Atopic dermatitis, pruritogens; brain-derived natriuretic peptide; pruritus; skin; dorsal root
87 ganglion; keratinocytes; dendritic cells; SNAREs

88

89

90

91

92

93

94

95

96

97

98

99

100 **ABBREVIATIONS USED**

101	AD	atopic dermatitis
102	BNP	brain-derived natriuretic peptide
103	<i>Calca</i>	calcitonin gene-related peptide (CGRP) gene
104	CCL20	C-C Motif Chemokine Ligand 20
105	CXCL	chemokine (C-X-C motif) ligand
106	DAPI	4',6-diamidino-2-phenylindole
107	DRGs	dorsal root ganglionic neurons
108	ET-1	endothelin-1
109	FPKM	fragments per kilobase of transcript per million mapped reads
110	GSK3	glycogen synthase kinase 3
111	hDCs	human dendritic cells
112	hKCs	human primary keratinocytes
113	HDM	house dust mite
114	IL-31	interleukin-31
115	IL-31RA	interleukin-31 receptor alpha
116	IL-31Tg mice	IL-31-transgenic mice
117	MMP9	plasma matrix metalloproteinase-9
118	NeuN antibody	NEURonal Nuclei antibody
119	<i>Nppb</i>	BNP gene
120	NPR1	natriuretic peptide receptor A
121	NPR2	natriuretic peptide receptor B
122	OSMR β	oncostatin M receptor beta subunit
123	PGP9.5	protein gene product 9.5
124	RT-PCR	real-time PCR
125	SNAP-25	synaptosomal associated protein 25k
126	SNARE	soluble N-ethylmaleimide-sensitive factor activating protein receptor
127	STX1	syntaxin 1
128	<i>Tac-1</i>	substance p (SP) gene
129	TG	trigeminal ganglia
130	Th2	T helper type 2
131	TSLP	thymic stromal lymphopoietin
132	VAMP	vesicle-associated membrane protein

133	V1	vesicle-associated membrane protein isoform 1
134	V7	vesicle-associated membrane protein isoform 7
135	WT	wild-type

ACCEPTED MANUSCRIPT

136 **INTRODUCTION**

137 Atopic dermatitis (AD) is one of the most prevalent chronic inflammatory skin diseases
138 world-wide. It is characterized by dysregulation of immunity, skin barrier as well as nerve
139 function, resulting clinically in eczema and itch (1-4). The mediators of histamine-
140 independent itch in AD are poorly understood (5). Candidates include endothelin-1 (ET-1),
141 thymic stromal lymphopoietin (TSLP) and the cytokines interleukin (IL)-4, IL-13 and IL-
142 31 (1). IL-31 is a critical cytokine in the pathophysiology of AD (1, 6, 7) playing a role in
143 eczema (7), itch (8), and nerve growth (9). Elevated serum levels of IL-31 were found to
144 correlate with disease severity in patients (6, 10). IL-31 serves as a critical neuron-immune
145 link between T helper type 2 (Th2) cells and sensory nerves in the generation of T cell-
146 mediated itch (8). Cutaneous and intrathecal injections of IL-31 evoked robust itch
147 behavior in mice (8). IL-31 injection in mouse cheek induces itch, but not pain (8). IL-31-
148 transgenic (Tg) mice that overexpress IL-31 develop severe pruritus and skin lesions
149 similar to AD (7). In mice, IL-31 receptor A (IL-31RA) associates with oncostatin M
150 receptor β (OSMR β) to form the IL-31RA heterodimeric complex that binds to IL-31 (8).
151 Targeting IL-31 pathway therapeutically has been proved to be effective in AD (11, 12).
152 For examples, IL-31 neutralization in AD-models was effective in the treatment of IL-31-
153 induced itch and dermatitis (13-17). Anti-IL-31RA antibody nemolizumab was evaluated in
154 phase II with satisfied efficacy and safety for the treatment of patients with moderate-to
155 severe AD disease (11). Despite this, it is not known if IL-31 stimulates neuropeptide
156 release from central and/or peripheral primary afferent neurons to modulate itch
157 transmission in skin and/or spinal cord. The importance of IL-31 in the regulation and
158 release of neuropeptides from peripheral sensory nerves in the skin and the resulting
159 neurogenic inflammation in AD, also remains elusive.

160 B-type natriuretic peptide (BNP) is a 32-amino-acid cyclic peptide expressed in a subset of
161 primary afferent neurons (18-20). It binds to the natriuretic peptide receptor A (NPR1) and
162 to a lesser extent NPR2 (21). BNP is the *Nppb* gene product and has been identified as an
163 important neuropeptide for itch transmission from the sensory to the spinal cord (19).
164 Intrathecal injection of BNP in mice induced a robust itch phenotype whereas *Nppb*^{-/-} mice
165 exhibited lack of scratching responses to many pruritogens (19). In contrast to substance P
166 (SP) and calcitonin gene-related peptide (CGRP) which facilitate pain processing and
167 painful neurogenic vasodilation in mice, BNP has been characterized as a negative
168 regulator of nociceptive transmission (20, 22). *Nppb* has been detected in the murine

169 primary puritogenic sensory dorsal root ganglionic neurons (DRGs), which overlapped with
170 IL-31RA⁺ neurons (23). Despite of its importance in itch, it is unknown whether BNP can
171 be released from peripheral sensory neurons in response to puritogens (i.e. IL-31 or
172 histamine). The cellular and molecular basis for its pruritic action on skin and immune cells
173 also remains unknown. Understanding the downstream signaling pathways of IL-31 and its
174 potential interacting mediators like BNP, CGRP or SP is significant because it will not only
175 expand our current knowledge and theoretical repertoire but may also aid the development
176 of a more efficacious treatment for chronic skin inflammation and pruritus. Herein, we
177 investigated the possible mechanistic relationship between IL-31 and BNP in itch. The aim
178 of the current study was to: (i) examine the expression and function of IL-31 receptor in
179 human DRGs (hDRGs); (ii) investigate the role of BNP in AD using mice models and
180 human subjects; (iii) investigate IL-31-induced release of BNP and other neuropeptides in
181 relation to itch; (iv) dissect the molecular components of the exocytotic machinery in IL-
182 31-induced BNP release; (v) study the alteration of BNP receptor in AD skin; (vi) screen
183 distinct intracellular kinases activated and cytokines induced by BNP in human skin cells.
184 Overall, our results reveal a novel IL-31-mediated downstream target in itch induction and
185 highlight the importance of BNP as a potential target for the treatment of AD and other itch
186 disorders.

187

188 **MATERIALS and METHODS**

189 **Materials**

190 Human skin samples from 3 donors of AD and 3 donors of healthy control subjects were
191 bought from Tissue Solutions Ltd., Glasgow, Scotland. Human DRG paraffin sections were
192 purchased from Amsbio (Local distributor of Zyagen Laboratories). Antibodies, cells and
193 reagents for tissue culture and others are detailed in the Supplementary Material and
194 Methods.

195

196 **Human and animal rights**

197 Human DRGs were isolated as previously described (24) with full legal consent by Anabios
198 Corporation (San Diego, CA, USA). DRGs were isolated and cultured from 1 donor (25
199 year old Hispanic female). Housing/handling of mice (C57BL6), IL-31Tg mice and
200 experimental procedures had been approved by the University College Dublin Ethics
201 Committee and the Irish Authorities. Housing/handling of Grhl3PAR2^{+/+} transgenic mice

202 model and experimental procedures following federal guidelines had been approved by the
203 University of California, San Francisco Ethics Committee and by local authorities.

204

205 **HDM application on Grhl3PAR2^{+/+} mouse model**

206 The Grhl3PAR2^{+/+} mice were maintained in C57BL6/J-129X1/SvJ mixed strain and used
207 for the experiments as an AD model. For details of HDM treatment, see Supplementary
208 Material and Methods.

209

210 **RNA-Seq**

211 For gene expression experiment, trigeminal ganglia (TG) were harvested from wild-type
212 (WT) and HDM-treated Grhl3PAR2^{+/+} mice and processed for RNA-Seq. For details, see
213 Supplementary Material and Methods.

214

215 **Quantitative real time PCR (RT-PCR)**

216 RNA was isolated from cultured mouse DRG neurons (mDRGs) using the RNeasy kit
217 (Qiagen, Hilden, Germany). TRIzol Reagent was used to isolate RNA from DRGs and
218 skins of WT and IL-31Tg mice. The quantitation of mRNA levels was performed by real
219 time fluorescence detection using SYBR Green ROX mix (ABI). For details, see
220 Supplementary Material and Methods.

221

222 **BNP, CGRP and SP release assay**

223 For detailed preparation of mDRGs culture and their release of neuropeptides, see
224 Supplementary Material and Methods.

225

226 **Measurement of intracellular Ca²⁺ concentration**

227 Human DRGs (hDRGs) and mDRGs in culture were loaded with calcium indicator before
228 measurement of Ca²⁺ mobilization in response to various pruritogens. For details, see
229 Supplementary Material and Methods.

230

231 **Immunofluorescence staining**

232 Cultured mDRGs, paraffin sections of human DRG and skin (15µm) were stained and
233 imaged by a Zeiss LSM710 confocal microscope (Carl Zeiss MicroImaging). For details,
234 see Supplementary Material and Methods.

235

236 **Lentivirus-mediated knockdown of soluble N-ethylmaleimide-sensitive factor**
237 **activating protein receptors (SNAREs)**

238 Cultured mDRGs in 7d *in vitro* were treated with non-targeted control lentiviral particles or
239 shRNA lentivirus specifically targeting to SNAREs for 7-10 days before measuring BNP
240 release and protein expression. For details, see Supplementary Material and Methods.

241

242 **Culture of human primary epidermal keratinocytes (hKCs) and human monocyte-**
243 **derived dendritic cells (hDCs), cytokine antibody array and phosphor-kinase array**

244 hKCs were cultured in the KBM-Gold™ medium with KBM-Gold SingleQuot KCs
245 supplement (Lonza). hDCs were cultured by *in vitro* differentiation of CD14⁺ monocytes
246 using LGM-3™ Lymphocyte Growth Medium plus 50 ng/ml GM-CSF and 50 ng/ml IL-4
247 (Lonza). Cells were maintained in the above medium for 3 d before use. For detailed
248 cytokine antibody and phosphor-kinase arrays, see Supplementary Material and Methods.

249

250 **Statistical Data Analysis**

251 Data expressed as mean ± S.E.M. n ≥ 3 independent experiments, probability values are
252 determined with the use of Student's 2-tailed t test; P values <0.05 are considered
253 significant; non-significant N.S. P>0.05; *P < 0.05; **P < 0.01; *** P<0.001. Data analysis
254 was performed with Prism software.

255

256 **RESULTS**

257

258 **IL-31RA and OSMRβ are co-expressed in a small subset of human DRG neurons**

259 In human AD, IL-31 levels correlate with disease severity (6, 10). However,
260 subpopulations responding to IL-31 and distribution of its receptors (IL-31RA and
261 OSMRβ) in hDRGs have not been fully characterized. Our study herein will help to define
262 the functional contribution of neuronal subpopulations to the skin inflammation of AD in
263 humans. Using double-immunohistochemistry, we observed IL-31RA and OSMRβ
264 expression in hDRG sections (Fig 1A-D). IL-31RA was detected in ~3% of total neurons
265 visualized with a neuronal marker NEUronal Nuclei (NeuN) antibody, which stained
266 strongly neuronal nuclei and distal cytoplasm (Fig 1A). IL-31RA also occurred in a small
267 proportion of cells immunoreactive to protein gene product 9.5 antibody (PGP9.5) (Fig 1B),
268 another marker for sensory nerves. Similarly, OSMRβ was found in a small subset of

269 PGP9.5⁺ neurons (Fig 1C). Co-staining of IL-31RA and OSMR β confirmed that in hDRG
270 all of IL-31RA⁺ neurons were OSMR β ⁺ (Fig 1D, E). However, ~5% OSMR β ⁺ neurons did
271 not appear to be strongly labeled by anti-IL-31RA (Fig 1D arrowed neuron).

272

273 **IL-31 induces intracellular calcium mobilization in a distinct subset of hDRGs, which**
274 **also responds to ET-1**

275 Functional identities of neuronal subsets were further assayed in hDRG using intracellular
276 Ca²⁺ imaging upon application of individual or combined puritogens to cultured hDRGs.
277 We found that ~4% hDRG neurons were directly activated by ET-1 (n=100 neurons) (Fig
278 2A, B top panels). The response consisted of a transient increase in intracellular calcium. In
279 comparison, glia cells consistently exhibited large responses with slow kinetic. In several
280 cases after ET-1 application, glial cells generated oscillatory calcium signals that persisted
281 even after the washout of ET-1 (Fig 2A, B top panels). In our observation, about ~50% of
282 neurons pre-exposed to ET-1 also responded to histamine (Fig 2A middle panel and C).
283 Following application of ET-1 and histamine some neurons exhibited spontaneous calcium
284 transients. Co-application of ET-1 and histamine did not potentiate the response. On the
285 contrary, de-sensitization was apparent in some neurons (Fig 2A bottom panel). For the IL-
286 31-induced response, 1 of 50 neurons pre-exposed to ET-1 responded with a rapid calcium
287 transient to IL-31 (Fig 2B top and middle panels). Likewise, co-application of ET-1 and IL-
288 31 did not potentiate the response, except in one neuron with a delayed response (Fig 2B
289 bottom panel). In summary, ~50% neurons responded to histamine, and ~4% of total
290 neurons responded to ET-1. Half of the ET-1-responsive neurons also responded to
291 histamine (Fig 2C). Overall, in hDRGs 2% of neurons were responding to IL-31, and these
292 cells also responded to ET-1 (Fig 2C). Due to the importance of IL-31 and ET-1 in
293 pathogenesis of AD, it is tempting to postulate that this neuronal subset mediates itch
294 transmission in humans.

295 We further investigated whether murine DRGs (mDRGs) exhibit similar phenomenon in
296 response to IL-31 and ET-1. Cultured mDRGs uploaded with Fluo-4AM were treated with
297 IL-31 and ET-1, sequentially. In a total of 335 neurons recorded, IL-31 activated 9 neurons
298 (~2.7%) and ET-1 activated 14 neurons (~4.2 %). 5 IL-31-responsive neurons did not
299 respond to ET-1 (Fig 2D.). Thus, similarities as well as differences were observed between
300 human and murine DRG with respect to IL-31 and ET-1 stimulation.

301

302 **PAR2 transgenic mice treated with house dust mite (HDM) and IL-31Tg mice are**
303 **associated with *Nppb* upregulation in sensory nerves**

304 We investigated the possible involvement of BNP in AD using Grhl3PAR2⁺ mice (25).
305 These mice develop atopic-like inflammation, scaly dry skin, epidermal hyperplasia, and
306 itch behaviors, all characteristics of human AD (25). We applied HDM on the right cheek
307 to induce severe dermatitis, as HDM have abundant proteases that can activate PAR2
308 constantly and stably. Ipsilateral (ipsi) and contralateral (contra) trigeminal ganglia (TG)
309 from each mouse were analyzed by RNA-Seq (Fig 3A). Clinical scores for pathologic
310 diagnosis (skin lesion severity) were evaluated by hematoxylin and eosin (HE) staining on
311 cheek skin biopsy from each of the 8 HDM-applied mice and vehicle-treated WT mice
312 (representative images shown in Fig 3B). Notably, in HDM-treated mice, the correlation
313 coefficient between clinical score and fold-change of fragments per kilobase of transcript
314 per million mapped reads (FPKM) for *Nppb* transcripts (ipsi/contra) is about 0.8 (Fig 3A).
315 Average of fold change of *Nppb* for these 8 mice is ~2.3. In contrast, HDM did not induce
316 significant change in TGs for NPR1, NPR2, IL-31, IL-31RA, and OSMR in Grhl3PAR2⁺
317 mice (Fig 3A). After comparing FPKM from TGs of ipsilateral (right cheek) vs
318 contralateral (left cheek) in 3 high clinical score Grhl3PAR2⁺ mice (score was 8, 7, 7), we
319 found that *Nppb* transcripts were upregulated by 3.5 times by application of HDM and
320 ranked the third position among the highly upregulated genes (Fig 3C). Notably, the *Nppb*
321 FPKM values in the contralateral (left) cheek of Grhl3PAR2⁺ mice were not significantly
322 different from that of WT mice with or without vehicle (Vaseline) treatment
323 (Supplementary Fig E1).

324 As IL-31Tg mice show skin phenotype closely resembling those of human AD (7), we used
325 RT-PCR to compare *Nppb* transcripts in whole DRG tissue isolated from the IL-31Tg
326 (lesional and non-lesional) and from age matched WT non-transgenic mice. Higher levels
327 of *Nppb* mRNA were detected in the DRGs isolated from both lesional and non-lesional IL-
328 31Tg mice (Fig 3D).

329 Collectively, our data indicate that BNP is implicated in AD and may be associated with
330 severity of AD-like skin conditions in mice.

331

332 **IL-31 augments release and upregulates synthesis of BNP but not CGRP or SP from**
333 **cultured mDRGs**

334 IL-31 directly activates peripheral sensory neurons to induce pruritus (8); however, its
335 effect on BNP has not yet been reported. To explore this possibility, we cultured mDRGs

336 and incubated neurons with 300 nM IL-31 for 30 min before starting the release assay. The
337 IL-31-induced release was compared with the response to histamine, high (HK, 60 mM) and
338 low (LK, 3.5 mM) potassium chloride buffers (Fig 4A). Notably, IL-31 elicited ~2.7 fold
339 increase of BNP release over the basal level (LK). Histamine (His) and potassium
340 depolarization (HK) also elicited BNP release (Fig 4A). Moreover, IL-31-induced BNP
341 release was concentration- (Fig 4B) and time- (Fig 4C) dependent. No significant
342 difference of BNP release (Fig 4B) and mRNA synthesis over 30 min (Supplementary Fig
343 E2 A) was detected between 300 nM and 1 μ M concentrations of IL-31. RT-PCR results
344 revealed that 300 nM IL-31 induced *Nppb* mRNA synthesis peaked at 4h and declined at 8h
345 (Supplementary Fig E2 B). In contrast, neither CGRP nor SP release was affected by IL-31
346 or His, although both were elicited by HK (Fig 4D). This finding demonstrates for the first
347 time that IL-31 directly activates sensory neurons to release BNP rather than CGRP or SP.
348 Consistently, incubation of mDRGs with IL-31 for 6h did not induce significant changes of
349 mRNA levels of *Calca* (CGRP gene) or *Tac-1* (SP gene) (Fig 4E). In contrast, IL-31
350 increased *Nppb* mRNA levels by ~2 fold. Altogether, these findings confirm that IL-31
351 directly induces BNP release and upregulates its synthesis, indicating BNP might
352 contribute to IL-31-mediated itch signaling.

353 Subsequently, we performed immunofluorescence studies using antibodies against BNP or
354 CGRP with their specificities verified (Supplementary Fig E3) to investigate their
355 expression and distribution pattern in mDRGs. Notably, BNP was expressed in both
356 CGRP⁺- and CGRP⁻- neurons (Fig 4F). This distinct, but overlapping distribution, suggests
357 that BNP and CGRP may have discrete functional roles in the transduction of itch
358 signaling.

359

360 **IL-31-induces BNP release from cultured mDRGs via a SNARE-mediated vesicle** 361 **fusion**

362 BNP release from sensory neurons in response to itch stimuli might be regulated by
363 selective exocytotic machinery. In terms of IL-31-induced BNP release, its mechanism is of
364 particular importance because of its relevance in AD. SNAREs are critical membrane
365 fusion proteins and serve as therapeutic targets for many neurological diseases (26). To
366 explore their role in BNP release, SNAP-25 (synaptosomal-associated protein 25k) and two
367 other vesicular SNARE proteins, vesicle-associated membrane protein (VAMP) isoform 1
368 (V1) and 7 (V7), were selectively knocked down using lentiviral shRNA particles.
369 Notably, expression levels of each protein were substantially reduced compared to the non-

370 targeted controls (Fig 5A). Knockdown of SNAP-25 and V1, but not V7, resulted in
371 complete blockade of IL-31-elicited BNP release (Fig 5B). These findings, for the first
372 time, demonstrated that selective SNARE proteins control IL-31-induced BNP release.

373

374 **Expression of BNP and its receptors is increased in the skin of patients with atopic** 375 **dermatitis**

376 To understand BNP-induced signaling and identify the functional consequence of BNP in
377 human skin level, we examined the expression of BNP and its receptor NPR1 and NPR2 in
378 cultured human keratinocytes (hKCs). Using immunostaining, we readily detected
379 expression of NPR1 and NPR2 in cultured hKCs (Supplementary Fig E4 A). Both receptors
380 showed punctate distribution. In a great contrast, BNP immune-signal was below the
381 detection limit in these cultured cells (Supplementary Fig E4 A).

382 Next, similar experiments were performed on human skin sections from AD subjects and
383 healthy controls. We found that in the epidermis, no staining of BNP was discernible in
384 normal skin, similar to the observation in cultured KCs, but it was readily detected in AD
385 skin (Fig 6A), indicating a disease-related upregulation of BNP expression. We also
386 detected immune-signals of NPR1 and NPR2 in the epidermal KCs of healthy skin (Fig
387 6A), and both signals were enhanced in AD skin (Fig 6A). We further analyzed the detailed
388 distribution of these receptors by taking high resolution confocal images in epidermal KCs.
389 Distinct localization of NPR1 and NPR2 were revealed in epidermal KCs of AD skin
390 sections. NPR1 predominantly resided along the plasma membrane of KCs, whereas NPR2
391 was detected both on plasmalemma and cytoplasm (Fig 6A). The enhanced labelling of
392 NPR1 and NPR2 might not be simply due to the acanthosis, because we did observe
393 increased immunoreactivity at single KC level by immunofluorescence staining.

394 We further investigated BNP, NPR1 and NPR2 expression in the dermis of human skin.
395 BNP expression was detected in the dermis of healthy skin, and its level appeared increased
396 in dermal structures including secretory portion of sweat glands and blood vessel of AD
397 skin (Fig 6B). Interestingly, NPR2 (Fig 6C, left panel) and NPR1 (not shown) did not seem
398 to colocalize with PGP9.5 in these structures. NPR1 and NPR2 co-occurred on the dermal
399 structures including secretory portion of sweat glands and blood vessel (Fig 6C middle and
400 right panels). There was no obvious incremental labelling of NPR1 or NPR2 in the dermal
401 structures (Fig 6C) and immune-reactive cells in AD skin compared to healthy skin
402 (Supplementary Fig E5).

403 Consistently, using RT-PCR we also found *Nppb* transcripts were upregulated in lesional
404 and non-lesional skin, compared with that in WT skin (Supplementary Fig E6 A).
405 Moreover, BNP receptor NPR1 mRNA level was also increased in the lesional skin from
406 IL-31Tg mice (Supplementary Fig E6 B).

407 Taken together, these collective data suggest that BNP might be involved in promoting the
408 dermatitis response through activated/upregulated receptor in AD.

409

410 **BNP induces release of IL-17A, chemokine (C-X-C motif) ligand 10 (CXCL10) and**
411 **matrix metalloproteinase 9 (MMP9) from cultured human keratinocytes through**
412 **activation of GSK3>JNK>ERK1/2>P38**

413 KCs of AD patients exhibit a propensity to produce exaggerated cytokines, chemokines and
414 proteases, which play major role in promoting and maintaining inflammation (27, 28).
415 However, nothing is known about the influence of BNP on hKCs. We firstly investigated
416 the possible BNP effect on hKCs. Cells in culture were exposed to BNP for 24 h before the
417 supernatant was collected and used for proteome profiler human XL cytokine array, which
418 allowed detecting 102 different cytokines simultaneously. An increase in IL-17A (~2.5
419 folds), CXCL10 (~2 fold), and to a lesser degree, MMP9 was detected in the culture
420 supernatant (Fig 7A). In contrast, significantly lower levels of cytokine release were
421 triggered by the same dose of SP. In comparison, incubation of hKCs with 1 μ M human
422 CGRP peptide for 24 h only induced minimal CXCL5 release (Fig 7A). IL-17A is a critical
423 cytokine involved in the pathogenesis of AD (29, 30). Its expression in KCs was reported
424 (31-33) and detected in our primary culture (Supplementary Fig E4 B). CXCL10 mediates
425 cell adhesion, migration and inflammatory infiltrates in AD (34). Elevated levels of IL-17A
426 and CXCL10 are implicated in patients with AD (28, 29, 35). Thus, peripheral BNP might
427 promote the release of itch-related cytokines by acting on the KCs to propagate itch signals
428 in AD.

429 Subsequently, we investigated the signaling pathways involved in the activation of the KCs
430 using phospho-kinase arrays on the cell lysate of hKCs harvested after exposure to 1 μ M
431 human BNP for 8 min. Glycogen synthase kinase 3 (GSK3), c-Jun N-terminal kinases
432 (JNK) pan (JNK kinase family includes three proteins named JNK1, 2, 3), ERK1/2 and P38
433 were significantly phosphorylated/activated by application of BNP. In contrast, ERK1/2,
434 JNK and to a lesser extent GSK3 were activated by SP (Fig 7B). IL-17A is considered to
435 be a potent stimulator of further inflammatory mediator production, amplifying the
436 inflammatory response. Therefore, using selective phosphor-kinase inhibitors, we

437 investigated which intracellular kinase was responsible for the BNP-mediated IL-17A
438 release from hKCs. 1 μ M P38 α inhibitor AL8697, GSK3 inhibitor SB216763 (inhibiting
439 the activity of α and β isozymes of GSK-3), or JNK inhibitor JNK-IN-8, were incubated
440 with cultured hKCs, for 1 h prior to and during 24 h incubation with BNP before
441 measuring IL-17A release using IL-17A ELISA kit. Inhibition of GSK3 by SB216763
442 abolished the IL-17A release, whereas AL8697 only gave minor blockade (Fig. 7C).
443 Because IL-17A is regarded as a key cytokine involved in the pathogenesis of AD (36, 37),
444 targeting GSK3 may prove effective for the inhibition of itch transmission.

445

446 **BNP stimulates release of CCL20 through c-Jun activation in human monocyte-** 447 **derived dendritic cells (hDCs)**

448 We then assess a possible functional consequence of BNP on skin immune cells, hDCs,
449 known to express BNP receptors (38). To do this, monocyte-derived hDCs were maintained
450 in the presence of IL-4 and GM-CSF to allow their differentiation before incubating with 1
451 μ M human BNP for 24 h. We found CCL20 release was increased significantly by BNP,
452 and this was not observed when incubated with 1 μ M SP (Fig 7D). In the phospho-kinase
453 array, BNP also activated c-Jun through phosphorylation, unlike SP which did not show
454 any effect on c-Jun activation (Fig 7E). CCL20 level is strongly increased in lesional skin
455 tissues with AD and it stimulates the migration of various immune cells (39-41). Thus,
456 BNP induction of CCL20 release may constitute a novel neuron-immuno-modulatory
457 mechanism that results in the activation of immature dendritic cells, which could contribute
458 to the persistent itch.

459

460 **DISCUSSION**

461 AD patients experience a ‘vicious cycle of itching and scratching’ (42). The molecular
462 basis for this phenomenon, however, is still unknown. Although it has recently been
463 revealed that cytokines like IL-31 and IL4 or IL-13 play a role in immunity and itch
464 transmission (8, 43, 44), it is currently unknown whether cytokines like IL-31 also regulate
465 neuropeptide release from peripheral nerve endings thereby modulating neurogenic
466 inflammation in AD (Fig 8). Understanding the importance of neuropeptide- and cytokine-
467 mediated intercellular communication would further explain not only the interplay between
468 inflammation and itch, but also how this debilitating symptomatology of inflammation and
469 itch may be therapeutically interrupted. Here, we show for the first time that peripherally

470 released BNP is implicated in AD pathophysiology through IL-31 stimulation and
471 subsequent regulation of cytokine, chemokine and MMP9 release. Moreover, we show
472 BNP also activates several major cell types in skin which are pivotal in AD itch
473 transmission such as keratinocytes and dendritic cells (Fig 8). Thus, we have revealed
474 another mechanism how TH2 cells simultaneously impact itch and neuro-inflammation.

475

476 BNP was originally identified as an important contributor of *central* itch being released
477 from central primary afferents to the dorsal horn of the spinal cord (19). Here we show for
478 the first time that BNP is released from peripheral nerve endings upon stimulation by
479 pruritogens like IL-31 and histamine. These findings provide a new link between Th2 cells,
480 mast cells and peripheral sensory nerves. Notably, this is unique to BNP as to other
481 neuropeptides, such as CGRP and SP, because neither of them are synthesized nor released
482 under the same conditions, despite both being linked to itch (45, 46). In addition, BNP
483 together with its receptor, NPR1, are expressed in CGRP⁺ small sensory neurons (47). In
484 fact, though traditionally viewed primarily as a pain mediator (48), SP has also been
485 implicated as an itch mediator in AD, with increased numbers of SP⁺-nerve fibers found
486 concomitantly with a decrease in cutaneous SP levels in lesional skin of AD (49, 50), and
487 responsiveness to the NK1R antagonist aprepitant (45, 51). In particular, BNP-expressing
488 sensory neurons are found not to be involved in acute, inflammatory or neuropathic pain
489 (19, 52), unlike SP and CGRP. Therefore, our findings further differentiate BNP from
490 CGRP and SP and highlight its importance in the neuropeptide-mediated pathogenesis of
491 AD-associated itch.

492

493 Here, we show for the first time that IL-31RA and OSMR β highly overlap in hDRGs,
494 similar to the results observed previously in mDRGs (53). Moreover, in hDRGs IL-31
495 elicited Ca²⁺-transient in ~50% ET-1-responsive neurons and ~2% of total neurons. Half of
496 ET-1-responsive neurons also responded to histamine. To our knowledge, this is the first
497 detailed characterization of human sensory sub-populations according their response to
498 sequential and combined pruritogens. In contrast, IL-31 and ET-1 excited partly
499 overlapping small subset of mDRG neurons. In response to IL-31, *Nppb* transcripts in
500 cultured mDRGs were specifically upregulated, but this was not found for *Tac-1* or *Calca*.
501 IL-31 was capable of eliciting ~2.7-fold increase of BNP release over the basal level. The
502 elicited release was completely dependent on particular SNARE proteins, SNAP-25 and

503 VAMP1, which are also important for several other inflammatory diseases (54). In contrast
504 to the minimal BNP release at resting condition, the IL-31-induced augmentation of
505 peripheral BNP release may link to excessive itch in AD induced by a positive feed-back
506 loop of amplifying itch mediators. This may also explain the difficulty to treat AD-
507 associated itch.

508

509 Using deep sequence, we detected upregulation of *Nppb* transcripts in isolated TGs from
510 the HDMs-treated PAR2 transgenic mice, which showed AD-like skin condition.
511 Furthermore, our data confirm that the *Nppb* gene is implicated in severe AD conditions
512 because mice with high clinical scores exhibit high levels of *Nppb* transcripts. Our findings
513 provided the first evidence showing a functional association of BNP with severity of AD.
514 Consistently, we established that *Nppb* transcripts in DRGs and skin of lesional IL-31Tg
515 mice were also greatly upregulated. NPR1 transcripts were increased in lesional IL-31Tg
516 skin. In fact, upregulation of BNP in murine AD-like skin has also been reported by a
517 recent finding using global transcriptome, which identified a significant *Nppb* upregulation
518 (>3 fold) in oxazolone-challenged AD-like dermatitis mice skin (55).

519 In a translational approach, we also provide evidence for the importance of BNP in AD
520 using skin from AD patient and healthy control subjects. We detected increased protein
521 levels of NPR1 and NPR2 in epidermis, particularly in KCs. Moreover, enhanced
522 expression of BNP in both epidermis and dermis of AD patient skin was revealed. In fact,
523 immunostaining signal of BNP, NPR1 and NPR2 protein seemed to be increased in single-
524 cell level of KCs; however, we could not exclude that the possibility of the acanthosis
525 might also contribute to the increment. The upregulated expression levels of BNP and its
526 receptors in AD patients suggest a role for the IL-31/BNP/BNPR-axis in peripheral itch
527 amplification in AD patients.

528

529 Although IL-31 rapidly induces itch in mice (7, 8) and is regarded as one of the major
530 'drivers' of itch in AD, it failed to induce immediate itch responses in humans as shown in
531 a recent study including both AD patients and healthy subjects monitored by skin prick
532 testing (56). Though there is a possibility of insufficient amount of IL-31 being
533 administered which failed to induce immediate itch response, the late onset of IL-31-
534 induced mild itch sensations might also be attributed to this cytokine exerting its pruritic
535 effect indirectly via KCs and secondary mediators, rather than by a sole action on its
536 receptors on cutaneous sensory nerves (56, 57). In addition, similar to IL-4 (44) IL-31 may

537 be a sensitizer in some patients and not a direct itch inducer. However, the variable
538 expression levels of IL-31 and IL-31RA in AD patients may explain that some patients will
539 respond more to IL-31 stimulation. Consequently, some patients may profit better from
540 Anti-IL-31 therapy than others (11, 12). It will be interesting to learn as to whether IL-4
541 and IL-13 are also linked to BNP release.

542 We demonstrate that BNP acts as the downstream skin-derived effector of IL-31. In
543 addition to its contribution to spinal processing of itch (19), excessive release of BNP from
544 peripheral sensory nerves stimulates NPR1 receptor to activate multiple intracellular
545 signaling pathways in skin, thereby contributing to skin inflammation in AD. We found
546 BNP activates GSK3 pathway and leads to the secretion of several important inflammatory
547 or itch modulators, such as IL-17A, CXCL10 or MMP9 from skin KCs. BNP activates C-
548 Jun to release CCL20 from DCs. All of these cytokines are known to be increased in AD
549 and represent an important potential component of the pathology of AD (58, 59).
550 Upregulation of BNP receptor(s) in turn, could further augment secretion of the above
551 important itch modulators from these cells. Thus, our results support a new pathway in
552 which BNP is a peripheral contributor of IL-31-mediated neurogenic inflammation in AD,
553 and establish the missing link between TH2-nerve mediated inflammation as well as
554 pruritus.

555

556 In conclusion, we describe a novel functional link between TH2 cells and sensory nerves
557 through IL-31 and BNP, and give first evidence between a functional association of
558 peripheral BNP in AD using human and rodent DRGs, animal models and patient skin in a
559 translational fashion. Indeed, Th2 cells, sensory neurons, keratinocytes and dendritic cells
560 release a complex network of cytokines and chemokines establishing a local milieu and
561 environment that favors AD skin inflammation. In this context, BNP seems to act as an
562 important “relay center” for peripheral and central itch circuits to facilitate itch, but also
563 neuroinflammation, in the pathogenesis of AD. We demonstrate that BNP acts through
564 multiple mechanisms: 1) IL-31 modulates pruriceptive neurons to rapidly induce SNARE-
565 dependent release of BNP, and 2) IL-31 increases the synthesis of *Nppb*; 3) BNP receptors
566 are upregulated in AD; 4) BNP signals through its upregulated receptors to directly activate
567 multiple intracellular kinases in skin cells to elicit the release of itch-related pro-
568 inflammatory cytokines (Fig 8). Our findings provide new insights about BNP as an
569 important regulator of neuro-inflammation as well as itch in the skin of AD, and close a
570 missing link why the itch inflammatory skin disease AD has been also defined as

571 'neurodermatitis'. In addition, peripheral BNP signaling provides a new basis for the
 572 development of more effective therapies for AD and probably other skin diseases.

573

574 **FIGURE LEGENDS**

575 **Fig 1. IL-31RA and OSMR β co-occurred in a small population of hDRGs. (A, B)**
 576 Representative immunofluorescence confocal images showing IL-31RA protein
 577 immunoreactivity only occurred in a subpopulation of neuronal cells in hDRG sections.
 578 Neuronal cells were stained by antibody against NeuN (A) or PGP9.5 (B). C, Co-staining
 579 of OSMR β with PGP9.5 in hDRG section. D, Immunofluorescence staining of hDRG
 580 section showing IL-31RA and OSMR β largely co-localised in a subset of neurons.
 581 Specimens were counterstained with DAPI to highlight all cell nuclei. Arrow pointed a
 582 neuron expressing OSMR β but not stained strongly by IL-31RA antibody. E, Venn
 583 diagram depicts the relationship of IL-31RA⁺, OSMR β ⁺ and NeuN⁺ populations in hDRG
 584 section. Total neuron numbers were counted based on the dual labelling of both NeuN and
 585 DAPI. A total of 573 cells were imaged.

586

587 **Fig 2. Puritogens-induced calcium mobilization and characterization of IL-31-**
 588 **responsive cells in hDRGs and mDRGs. A,** Representative traces for calcium
 589 measurement after sequential pruritogen mediators application. Traces show individual cell
 590 responding to ET-1 only (top), histamine only (middle), ET-1 plus histamine (bottom).
 591 Notably, there are some ET-1-responsive neurons that also responded to histamine. **B,**
 592 Neurons responding to ET-1 only (top), IL-31 only (middle), ET-1 plus IL-31 (bottom). **C,**
 593 Venn diagrams for percentage of neurons that responded to puritogenic compounds. Total
 594 number of hDRGs recorded=100. **D.** Four representative traces of mDRG cells responsive
 595 to IL-31 and/or ET-1. Note that cell 1 responded to both IL-31 and ET-1; cell 2 only
 596 responded to ET-1, whereas cell 3 failed to respond to either IL-31 or ET-1; cell 4 is an IL-
 597 31-responsive cell which did not respond to ET-1. Venn diagram showing relative
 598 proportions of mDRG neurons responsive to IL-31 and/or ET-1. A total of 335 mDRGs
 599 were recorded.

600

601 **Fig 3. *Nppb* is upregulated in sensory ganglia from HDM-treated *Grhl3PAR2*^{+/+} mice**
 602 **and IL-31Tg mice. A,** The FPKM for *Nppb*, NPR1, NPR2, IL-31, IL-31RA and OSMR
 603 gene from TGs of ipsilateral vs contralateral (ipsi vs contra) were analyzed by RNA-seq

604 and compared. Eight mice were treated with HDM on the right cheek and nothing on the
 605 left cheek, and the cheek biopsies were clinical scored using HE staining. Correlation
 606 coefficient between clinical score and fold change of *Nppb* is about 0.8, whereas for other
 607 genes analyzed the values are not significant. For these 8 mice the average of fold change
 608 of *Nppb* is 2.3. **B**, Representative HE staining images showing the severity of skin lesion
 609 from HDM-treated mice, compared with vehicle-treated WT control. Images were taken by
 610 10x magnification objective. **C**, FPKM analyzed by RNA-seq of the top 3 high clinical
 611 score mice (Score is 8, 7 and 7) show the *Nppb* gene was upregulated by 3.5 times (ipsi vs
 612 contra). Average of fold change for genes upregulated and reached significance were
 613 plotted. A two-fold change in FPKM was deemed significant. **D**, RT-PCR analysis of
 614 *Nppb* mRNA levels in DRGs isolated from lesional, non-lesional IL-31Tg or WT mice.
 615 Values were normalized to the housekeeping gene GADPH. The results (mean \pm S.E.M.)
 616 are pooled data from multiple animals. Significant difference is indicated; * $P < 0.05$; **
 617 $P < 0.01$.

618

619 **Fig 4. IL-31 induces the release and mRNA synthesis of BNP (but not CGRP or SP)**
 620 **from cultured mDRGs.** Release of BNP (**A**), CGRP and SP (**D**) over 30 min was
 621 measured by their specific ELISA or EIA, and the increment of release after each treatment
 622 was plotted relative to the basal level. The amount in pg/ml in basal (LK) release is: $15.3 \pm$
 623 1.2 for BNP; 3.9 ± 0.9 for SP; 49.3 ± 11.8 for CGRP. LK, low potassium basal buffer; HK,
 624 high potassium stimulation buffer; HIS, histamine. **B**, BNP release induced by various
 625 dose of IL-31 over 30 min. **C**, Time-dependence of BNP release induced by 300 nM IL-31.
 626 **E**, RT-PCR for mRNA of *Nppb*, *Calca* and *Tac-1* in cultured mDRGs after treatment with
 627 100ng/ml IL-31 for 6h. Data in **A –E** are presented as mean \pm S.E.M. $n \geq 3$ independent
 628 experiments. Significant difference is indicated; N.S. $P > 0.05$; * $P < 0.05$; ** $P < 0.01$; ***
 629 $P < 0.001$. **F**, Immunofluorescence study for cellular localization of CGRP (red) and BNP
 630 (green) after dual labelling of DRGs with each specific antibody and counterstained with
 631 DAPI (blue). Scale bars are indicated.

632

633 **Fig 5. IL-31-induced BNP release from cultured mDRGs requires SNARE proteins.** **A**,
 634 Representative immunoblots show knock-down of SNAP-25 (S25), VAMP1 (V1) and
 635 VAMP7 (V7) protein expression in cultured DRGs using lentiviral shRNA particles.
 636 Syntaxin 1 (STX1) serves as an internal control in each blot. Non-targeted virus-treated
 637 samples were loaded to the gels for the comparison. **B**, Quantified plot demonstrates that

638 300 nM IL-31-elicited BNP release over 30min is inhibited after knockdown of S25 and V1
639 but not V7. Data are presented as mean \pm S.E.M. $n \geq 3$ independent experiments.
640 Significant difference between specific shRNA-treated cells and non-targeted controls is
641 indicated; N.S. $P > 0.05$; *** $P < 0.001$.

642

643 **Fig 6. Immunohistochemical staining of BNP, NPR1 and NPR2 in the skin of human**
644 **healthy control and AD patient. A.** Representative fluorescent images show expression
645 patterns of BNP, NPR1 and NPR2 in AD and healthy control skin. Note that epidermal
646 keratinocytes layer of AD skin showed enhanced staining of BNP, NPR1 and NPR2
647 compared to healthy control skin. Boxed areas in the middle panels are shown at higher
648 magnification in right panels. **B.** Images show increased BNP staining in the dermal
649 structures including secretory portion of sweat glands and blood vessel in AD skin
650 compared with the healthy skin. **C.** NPR2 does not co-localize with nerve marker PGP9.5
651 in the dermal structures, but highly co-localizes with NPR1. There is no obvious change of
652 NPR1 and NPR2 expression in dermis between AD patient skin and control healthy skin.
653 Scale bars are indicated. Paraffin-embedded human skin sections ($n=10$) from each donor
654 of AD and healthy control subjects were stained for each condition. The white dotted lines
655 denote the epidermal–dermal junctions.

656

657 **Fig 7. Effect of BNP on cytokine/chemokine release and activation of intracellular**
658 **phosphor-kinase. A,** Release profile of cytokines from cultured hKCs detected by
659 antibody array. Data from BNP-, SP- or CGRP-induced release were calculated relative to
660 non-treated control (basal). **B,** Neuropeptide-induced activation of intracellular phosphor-
661 kinases. Data plotted are the ratio of phosphorylated signal obtained from neuropeptide-
662 treated cells relative to non-treated control. **C,** Percentages of inhibition by selective kinase
663 inhibitors of BNP-induced IL-17A release from hKCs. **D,** CCL20 release from cultured
664 hDCs induced by BNP or SP. **E,** Phosphorylation of intracellular c-Jun from hDCs after
665 incubation with BNP or SP. Data are presented as mean \pm S.E.M. $n \geq 3$ independent
666 experiments. Significant difference between stimulated and basal is indicated; * $P < 0.05$; **
667 $P < 0.01$; *** $P < 0.001$.

668

669 **Fig 8. Schematic diagram illustrates an important communication link between IL-31**
670 **and BNP, both of which are key players in the signaling pathways implicated in**
671 **pruritus.** Itch inducers such as IL-31 and histamine elicit BNP release via SNARE-

672 controlled mechanism. Augmented release and synthesis by IL-31 of BNP might contribute
673 to central and peripheral itch signaling. In contrast, CGRP and SP are not elicited by these
674 puritogens. Released BNP subsequently increases IL-17A, CXCL10 and MMP9 release
675 from keratinocytes; however, SP and CGRP only elicit minimum release of CXCL10 and
676 CXCL5, respectively. BNP also mediates CCL20 from dendritic cells. Taken together, it is
677 postulated that these released cytokines/chemokines modulate itch transmission and
678 pathogenesis of AD.

679

680 **DECLARATION OF INTEREST**

681 We declare no conflict of interest.

682 **Reference**

- 683 1. Bieber T. Atopic dermatitis. *The New England journal of medicine*.
684 2008;358(14):1483-94.
- 685 2. Weidinger S, and Novak N. Atopic dermatitis. *Lancet*. 2016;387(10023):1109-
686 22.
- 687 3. Steinhoff M, Bienenstock J, Schmelz M, Maurer M, Wei E, and Biro T.
688 Neurophysiological, neuroimmunological, and neuroendocrine basis of
689 pruritus. *The Journal of investigative dermatology*. 2006;126(8):1705-18.
- 690 4. Roosterman D, Goerge T, Schneider SW, Bunnett NW, and Steinhoff M.
691 Neuronal control of skin function: the skin as a neuroimmunoendocrine organ.
692 *Physiological reviews*. 2006;86(4):1309-79.
- 693 5. Buddenkotte J, and Steinhoff M. Pathophysiology and therapy of pruritus in
694 allergic and atopic diseases. *Allergy*. 2010;65(7):805-21.
- 695 6. Sonkoly E, Muller A, Lauerma AI, Pivarcsi A, Soto H, Kemeny L, Alenius H, Dieu-
696 Nosjean MC, Meller S, Rieker J, et al. IL-31: a new link between T cells and
697 pruritus in atopic skin inflammation. *The Journal of allergy and clinical*
698 *immunology*. 2006;117(2):411-7.
- 699 7. Dillon SR, Sprecher C, Hammond A, Bilsborough J, Rosenfeld-Franklin M,
700 Presnell SR, Haugen HS, Maurer M, Harder B, Johnston J, et al. Interleukin 31, a
701 cytokine produced by activated T cells, induces dermatitis in mice. *Nature*
702 *immunology*. 2004;5(7):752-60.
- 703 8. Cevikbas F, Wang X, Akiyama T, Kempkes C, Savinko T, Antal A, Kukova G, Buhl
704 T, Ikoma A, Buddenkotte J, et al. A sensory neuron-expressed IL-31 receptor
705 mediates T helper cell-dependent itch: Involvement of TRPV1 and TRPA1. *The*
706 *Journal of allergy and clinical immunology*. 2014;133(2):448-60.
- 707 9. Feld M, Garcia R, Buddenkotte J, Katayama S, Lewis K, Muirhead G, Hevezi P,
708 Plessner K, Schrupf H, Krjutskov K, et al. The pruritus- and TH2-associated
709 cytokine IL-31 promotes growth of sensory nerves. *The Journal of allergy and*
710 *clinical immunology*. 2016;138(2):500-8 e24.
- 711 10. Raap U, Weissmantel S, Gehring M, Eisenberg AM, Kapp A, and Folster-Holst R.
712 IL-31 significantly correlates with disease activity and Th2 cytokine levels in
713 children with atopic dermatitis. *Pediatric allergy and immunology : official*

- 714 *publication of the European Society of Pediatric Allergy and Immunology.*
715 2012;23(3):285-8.
- 716 11. Ruzicka T, Hanifin JM, Furue M, Pulka G, Mlynarczyk I, Wollenberg A, Galus R,
717 Etoh T, Mihara R, Yoshida H, et al. Anti-Interleukin-31 Receptor A Antibody for
718 Atopic Dermatitis. *The New England journal of medicine.* 2017;376(9):826-35.
- 719 12. Ruzicka T, and Mihara R. Anti-Interleukin-31 Receptor A Antibody for Atopic
720 Dermatitis. *The New England journal of medicine.* 2017;376(21):2093.
- 721 13. Michels GM, Walsh KF, Kryda KA, Mahabir SP, Walters RR, Hoevers JD, and
722 Martinon OM. A blinded, randomized, placebo-controlled trial of the safety of
723 lokivetmab (ZTS-00103289), a caninized anti-canine IL-31 monoclonal
724 antibody in client-owned dogs with atopic dermatitis. *Veterinary dermatology.*
725 2016;27(6):505-e136.
- 726 14. Michels GM, Ramsey DS, Walsh KF, Martinon OM, Mahabir SP, Hoevers JD,
727 Walters RR, and Dunham SA. A blinded, randomized, placebo-controlled, dose
728 determination trial of lokivetmab (ZTS-00103289), a caninized, anti-canine IL-
729 31 monoclonal antibody in client owned dogs with atopic dermatitis.
730 *Veterinary dermatology.* 2016;27(6):478-e129.
- 731 15. Kasutani K, Fujii E, Ohyama S, Adachi H, Hasegawa M, Kitamura H, and
732 Yamashita N. Anti-IL-31 receptor antibody is shown to be a potential
733 therapeutic option for treating itch and dermatitis in mice. *British journal of*
734 *pharmacology.* 2014;171(22):5049-58.
- 735 16. Grimstad O, Sawanobori Y, Vestergaard C, Bilsborough J, Olsen UB, Gronhoj-
736 Larsen C, and Matsushima K. Anti-interleukin-31-antibodies ameliorate
737 scratching behaviour in NC/Nga mice: a model of atopic dermatitis.
738 *Experimental dermatology.* 2009;18(1):35-43.
- 739 17. Bilsborough J, Mudri S, Chadwick E, Harder B, and Dillon SR. IL-31 receptor (IL-
740 31RA) knockout mice exhibit elevated responsiveness to oncostatin M. *Journal*
741 *of immunology.* 2010;185(10):6023-30.
- 742 18. Bautista DM, Wilson SR, and Hoon MA. Why we scratch an itch: the molecules,
743 cells and circuits of itch. *Nature neuroscience.* 2014;17(2):175-82.
- 744 19. Mishra SK, and Hoon MA. The cells and circuitry for itch responses in mice.
745 *Science.* 2013;340(6135):968-71.
- 746 20. Liu XY, Wan L, Huo FQ, Barry DM, Li H, Zhao ZQ, and Chen ZF. B-type
747 natriuretic peptide is neither itch-specific nor functions upstream of the GRP-
748 GRPR signaling pathway. *Molecular pain.* 2014;10(4).
- 749 21. Matsukawa N, Grzesik WJ, Takahashi N, Pandey KN, Pang S, Yamauchi M, and
750 Smithies O. The natriuretic peptide clearance receptor locally modulates the
751 physiological effects of the natriuretic peptide system. *Proceedings of the*
752 *National Academy of Sciences of the United States of America.*
753 1999;96(13):7403-8.
- 754 22. Zhang FX, Liu XJ, Gong LQ, Yao JR, Li KC, Li ZY, Lin LB, Lu YJ, Xiao HS, Bao L, et
755 al. Inhibition of inflammatory pain by activating B-type natriuretic peptide
756 signal pathway in nociceptive sensory neurons. *The Journal of neuroscience :*
757 *the official journal of the Society for Neuroscience.* 2010;30(32):10927-38.
- 758 23. Li CL, Li KC, Wu D, Chen Y, Luo H, Zhao JR, Wang SS, Sun MM, Lu YJ, Zhong YQ,
759 et al. Somatosensory neuron types identified by high-coverage single-cell RNA-
760 sequencing and functional heterogeneity. *Cell research.* 2016;26(1):83-102.

- 761 24. Davidson S, Copits BA, Zhang J, Page G, Ghetti A, and Gereau RWt. Human
762 sensory neurons: Membrane properties and sensitization by inflammatory
763 mediators. *Pain*. 2014;155(9):1861-70.
- 764 25. Frateschi S, Camerer E, Crisante G, Rieser S, Membrez M, Charles RP, Beermann
765 F, Stehle JC, Breiden B, Sandhoff K, et al. PAR2 absence completely rescues
766 inflammation and ichthyosis caused by altered CAP1/Prss8 expression in
767 mouse skin. *Nature communications*. 2011;2(161).
- 768 26. Meng J, and Wang J. Role of SNARE proteins in tumourigenesis and their
769 potential as targets for novel anti-cancer therapeutics. *Biochimica et biophysica*
770 *acta*. 2015;1856(1):1-12.
- 771 27. Albanesi C, Scarponi C, Giustizieri ML, and Girolomoni G. Keratinocytes in
772 inflammatory skin diseases. *Current drug targets Inflammation and allergy*.
773 2005;4(3):329-34.
- 774 28. Giustizieri ML, Mascia F, Frezzolini A, De Pita O, Chinni LM, Giannetti A,
775 Girolomoni G, and Pastore S. Keratinocytes from patients with atopic
776 dermatitis and psoriasis show a distinct chemokine production profile in
777 response to T cell-derived cytokines. *The Journal of allergy and clinical*
778 *immunology*. 2001;107(5):871-7.
- 779 29. Koga C, Kabashima K, Shiraishi N, Kobayashi M, and Tokura Y. Possible
780 pathogenic role of Th17 cells for atopic dermatitis. *The Journal of investigative*
781 *dermatology*. 2008;128(11):2625-30.
- 782 30. Toda M, Leung DY, Molet S, Boguniewicz M, Taha R, Christodoulopoulos P,
783 Fukuda T, Elias JA, and Hamid QA. Polarized in vivo expression of IL-11 and IL-
784 17 between acute and chronic skin lesions. *The Journal of allergy and clinical*
785 *immunology*. 2003;111(4):875-81.
- 786 31. Li ZJ, Choi DK, Sohn KC, Lim SK, Im M, Lee Y, Seo YJ, Kim CD, and Lee JH.
787 Induction of Interleukin-22 (IL-22) production in CD4+ T Cells by IL-17A
788 Secreted from CpG-Stimulated Keratinocytes. *Annals of dermatology*.
789 2016;28(5):579-85.
- 790 32. Yu J, Xiao Z, Zhao R, Lu C, and Zhang Y. Paeoniflorin suppressed IL-22 via p38
791 MAPK pathway and exerts anti-psoriatic effect. *Life sciences*. 2017;180(17-22).
- 792 33. An J, Li T, Dong Y, Li Z, and Huo J. Terminalia Chebunanin Attenuates Psoriatic
793 Skin Lesion via Regulation of Heme Oxygenase-1. *Cellular physiology and*
794 *biochemistry : international journal of experimental cellular physiology,*
795 *biochemistry, and pharmacology*. 2016;39(2):531-43.
- 796 34. Flier J, Boorsma DM, van Beek PJ, Nieboer C, Stoof TJ, Willemze R, and Tensen
797 CP. Differential expression of CXCR3 targeting chemokines CXCL10, CXCL9, and
798 CXCL11 in different types of skin inflammation. *The Journal of pathology*.
799 2001;194(4):398-405.
- 800 35. Kolls JK, and Linden A. Interleukin-17 family members and inflammation.
801 *Immunity*. 2004;21(4):467-76.
- 802 36. Kirkham BW, Kavanaugh A, and Reich K. Interleukin-17A: a unique pathway in
803 immune-mediated diseases: psoriasis, psoriatic arthritis and rheumatoid
804 arthritis. *Immunology*. 2014;141(2):133-42.
- 805 37. Dhingra N, and Guttman-Yassky E. A possible role for IL-17A in establishing
806 Th2 inflammation in murine models of atopic dermatitis. *The Journal of*
807 *investigative dermatology*. 2014;134(8):2071-4.
- 808 38. Morita R, Ukyo N, Furuya M, Uchiyama T, and Hori T. Atrial natriuretic peptide
809 polarizes human dendritic cells toward a Th2-promoting phenotype through

- 810 its receptor guanylyl cyclase-coupled receptor A. *Journal of immunology*.
811 2003;170(12):5869-75.
- 812 39. Campbell JJ, Hedrick J, Zlotnik A, Siani MA, Thompson DA, and Butcher EC.
813 Chemokines and the arrest of lymphocytes rolling under flow conditions.
814 *Science*. 1998;279(5349):381-4.
- 815 40. Dieu MC, Vanbervliet B, Vicari A, Bridon JM, Oldham E, Ait-Yahia S, Briere F,
816 Zlotnik A, Lebecque S, and Caux C. Selective recruitment of immature and
817 mature dendritic cells by distinct chemokines expressed in different anatomic
818 sites. *The Journal of experimental medicine*. 1998;188(2):373-86.
- 819 41. Krzysiek R, Lefevre EA, Bernard J, Foussat A, Galanaud P, Louache F, and
820 Richard Y. Regulation of CCR6 chemokine receptor expression and
821 responsiveness to macrophage inflammatory protein-3 α /CCL20 in human
822 B cells. *Blood*. 2000;96(7):2338-45.
- 823 42. Steinhoff M, Cevikbas F, Yeh I, Chong K, Buddenkotte J, and Ikoma A. Evaluation
824 and management of a patient with chronic pruritus. *The Journal of allergy and
825 clinical immunology*. 2012;130(4):1015-6 e7.
- 826 43. Oh MH, Oh SY, Lu J, Lou H, Myers AC, Zhu Z, and Zheng T. TRPA1-dependent
827 pruritus in IL-13-induced chronic atopic dermatitis. *Journal of immunology*.
828 2013;191(11):5371-82.
- 829 44. Oetjen LK, Mack MR, Feng J, Whelan TM, Niu H, Guo CJ, Chen S, Trier AM, Xu AZ,
830 Tripathi SV, et al. Sensory Neurons Co-opt Classical Immune Signaling
831 Pathways to Mediate Chronic Itch. *Cell*. 2017;171(1):217-28 e13.
- 832 45. Azimi E, Reddy VB, Pereira PJ, Talbot S, Woolf CJ, and Lerner EA. Substance P
833 activates Mas-related G protein-coupled receptors to induce itch. *The Journal of
834 allergy and clinical immunology*. 2017.
- 835 46. Andoh T, Nagasawa T, Satoh M, and Kuraishi Y. Substance P induction of itch-
836 associated response mediated by cutaneous NK1 tachykinin receptors in mice.
837 *The Journal of pharmacology and experimental therapeutics*. 1998;286(3):1140-
838 5.
- 839 47. Marchenkova A, Vilotti S, Fabbretti E, and Nistri A. Brain Natriuretic Peptide
840 Constitutively Downregulates P2X3 Receptors by Controlling their
841 Phosphorylation State and Membrane Localization. *Molecular pain*.
842 2015;11(71).
- 843 48. Neumann S, Doubell TP, Leslie T, and Woolf CJ. Inflammatory pain
844 hypersensitivity mediated by phenotypic switch in myelinated primary
845 sensory neurons. *Nature*. 1996;384(6607):360-4.
- 846 49. Fantini F, Pincelli C, Romualdi P, Donatini A, and Giannetti A. Substance P levels
847 are decreased in lesional skin of atopic dermatitis. *Experimental dermatology*.
848 1992;1(3):127-8.
- 849 50. Giannetti A, Fantini F, Cimitan A, and Pincelli C. Vasoactive intestinal
850 polypeptide and substance P in the pathogenesis of atopic dermatitis. *Acta
851 dermato-venereologica Supplementum*. 1992;176(90-2).
- 852 51. Stander S, Siepmann D, Herrgott I, Sunderkotter C, and Luger TA. Targeting the
853 neurokinin receptor 1 with aprepitant: a novel antipruritic strategy. *PloS one*.
854 2010;5(6):e10968.
- 855 52. Pitake S, Debrecht J, and Mishra SK. [EXPRESS] Brain natriuretic peptide (BNP)
856 expressing sensory neurons are not involved in acute, inflammatory or
857 neuropathic pain. *Molecular pain*. 2017;13(1744806917736993).

- 858 53. Bando T, Morikawa Y, Komori T, and Senba E. Complete overlap of interleukin-
859 31 receptor A and oncostatin M receptor beta in the adult dorsal root ganglia
860 with distinct developmental expression patterns. *Neuroscience*.
861 2006;142(4):1263-71.
- 862 54. Meng J, Wang J, Lawrence G, and Dolly JO. Synaptobrevin I mediates exocytosis
863 of CGRP from sensory neurons and inhibition by botulinum toxins reflects their
864 anti-nociceptive potential. *Journal of cell science*. 2007;120(Pt 16):2864-74.
- 865 55. Ewald DA, Noda S, Oliva M, Litman T, Nakajima S, Li X, Xu H, Workman CT,
866 Scheipers P, Svitacheva N, et al. Major differences between human atopic
867 dermatitis and murine models, as determined by using global transcriptomic
868 profiling. *The Journal of allergy and clinical immunology*. 2017;139(2):562-71.
- 869 56. Hawro T, Saluja R, Weller K, Altrichter S, Metz M, and Maurer M. Interleukin-31
870 does not induce immediate itch in atopic dermatitis patients and healthy
871 controls after skin challenge. *Allergy*. 2014;69(1):113-7.
- 872 57. Cheung PF, Wong CK, Ho AW, Hu S, Chen DP, and Lam CW. Activation of human
873 eosinophils and epidermal keratinocytes by Th2 cytokine IL-31: implication for
874 the immunopathogenesis of atopic dermatitis. *International immunology*.
875 2010;22(6):453-67.
- 876 58. Harper JI, Godwin H, Green A, Wilkes LE, Holden NJ, Moffatt M, Cookson WO,
877 Layton G, and Chandler S. A study of matrix metalloproteinase expression and
878 activity in atopic dermatitis using a novel skin wash sampling assay for
879 functional biomarker analysis. *The British journal of dermatology*.
880 2010;162(2):397-403.
- 881 59. Kanda N, Shimizu T, Tada Y, and Watanabe S. IL-18 enhances IFN-gamma-
882 induced production of CXCL9, CXCL10, and CXCL11 in human keratinocytes.
883 *European journal of immunology*. 2007;37(2):338-50.
884

Fig. 1

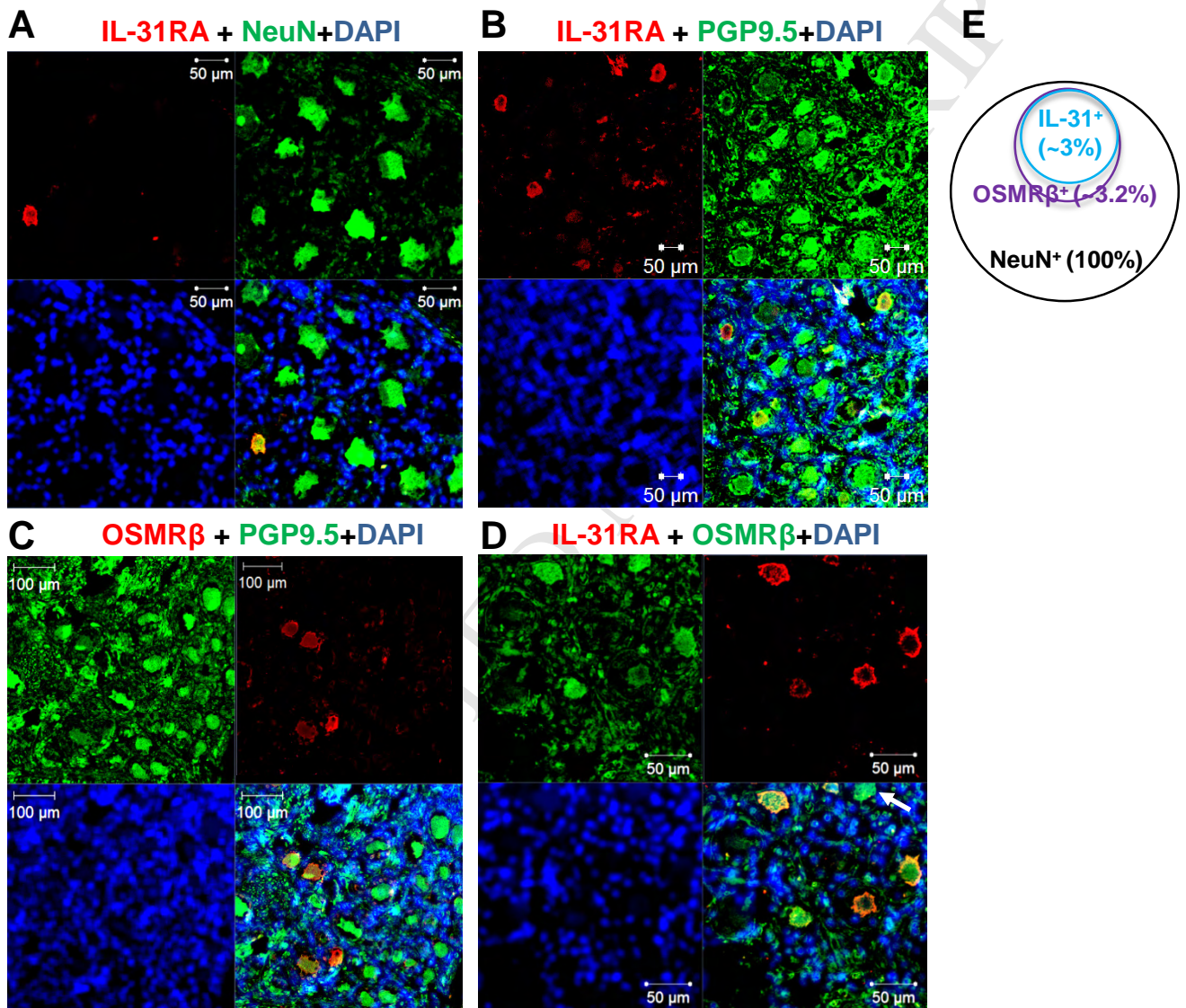


Fig. 2

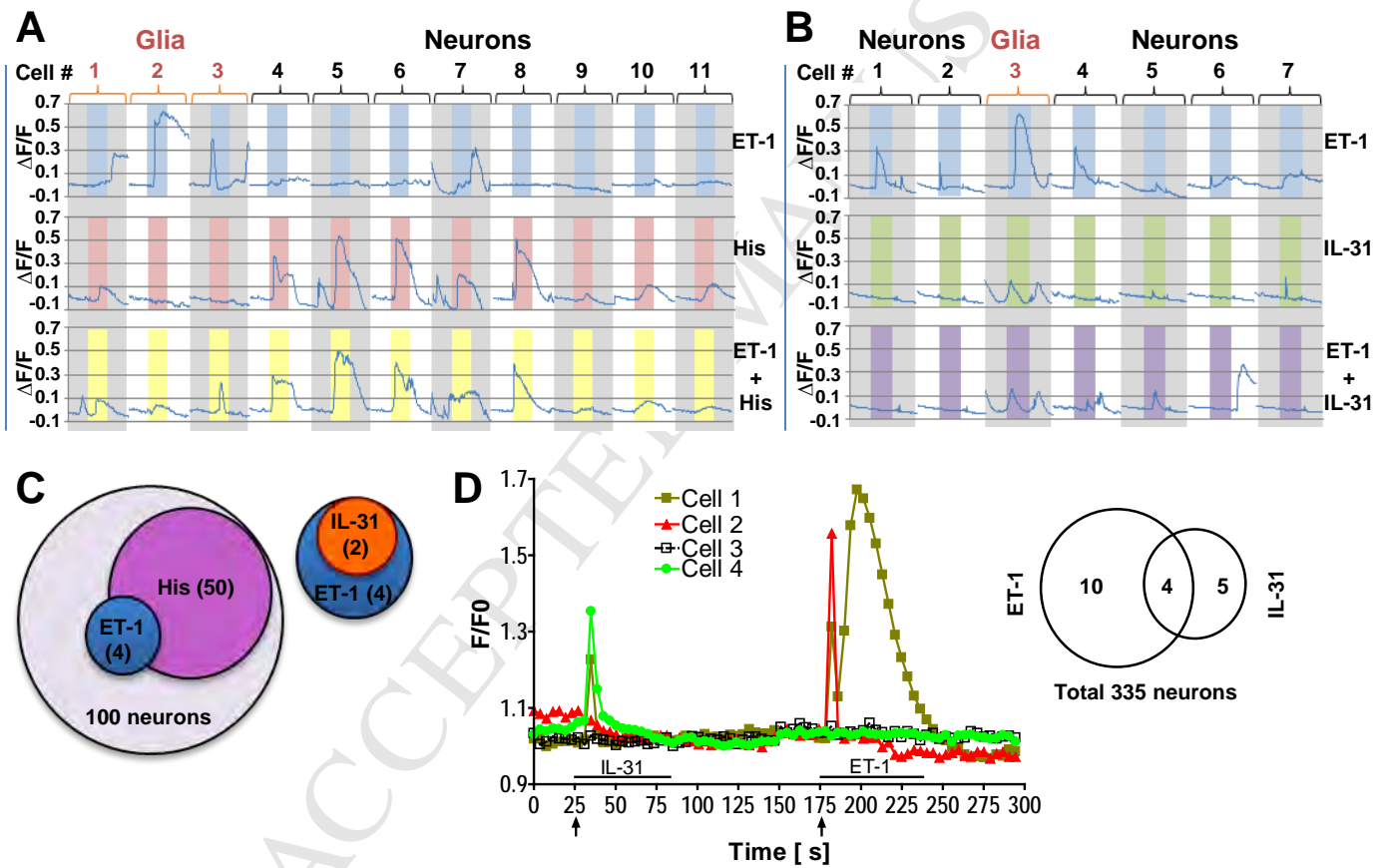


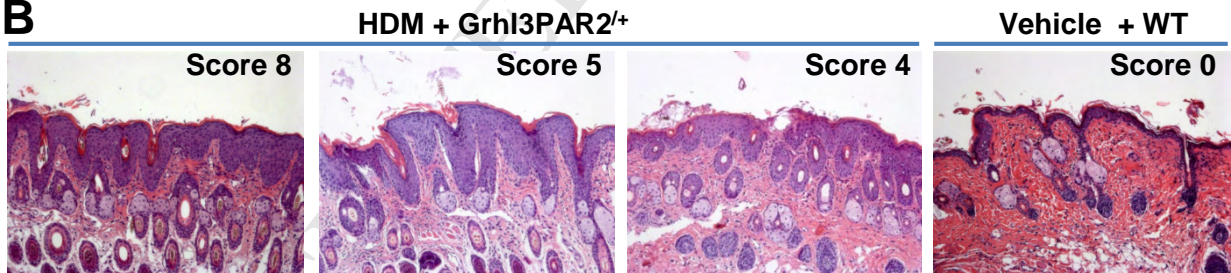
Fig. 3

A

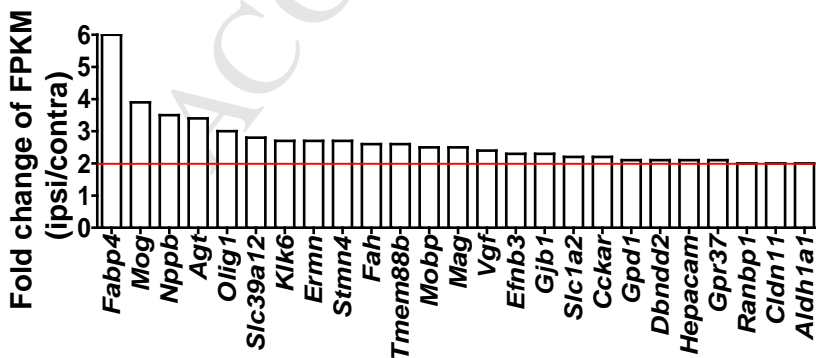
Nppb				NPR1				NPR2			
Clinical Score	FPKM		ipsi/contra	Clinical Score	FPKM		ipsi/contra	Clinical Score	FPKM		ipsi/contra
	ipsi	contra	Fold Change		ipsi	contra	Fold Change		ipsi	contra	Fold Change
8	21.1	8.7	2.4	8	0.5	0.7	0.6	8	15.2	13.4	1.1
7	17.6	3.9	4.5	7	0.6	0.3	2.4	7	14.6	14.9	1.0
7	29.4	7.7	3.8	7	0.8	1.2	0.7	7	15.9	14.0	1.1
5	19.7	8.1	2.4	5	1.0	0.7	1.3	5	11.8	14.5	0.8
4	10.2	8.8	1.2	4	1.1	0.7	1.5	4	16.1	15.0	1.1
3	20.0	12.2	1.6	3	0.4	0.3	1.2	3	15.7	14.5	1.1
3	12.5	6.8	1.8	3	0.7	0.3	2.2	3	21.1	15.5	1.4
2	5.4	13.4	0.4	2	1.4	0.6	2.5	2	19.1	18.8	1.0
correlation coefficient			0.799	correlation coefficient			-0.556	correlation coefficient			-0.126

IL-31				IL-31RA				OSMR			
Clinical Score	FPKM		ipsi/contra	Clinical Score	FPKM		ipsi/contra	Clinical Score	FPKM		ipsi/contra
	ipsi	contra	Fold Change		ipsi	contra	Fold Change		ipsi	contra	Fold Change
8	0.0	0.0	-	8	3.6	4.4	0.8	8	17.5	20.0	0.9
7	0.0	0.0	-	7	1.6	2.2	0.7	7	15.0	10.1	1.5
7	0.0	0.0	-	7	3.5	4.4	0.8	7	16.3	13.3	1.2
5	0.0	0.0	-	5	2.5	2.2	1.1	5	13.8	14.3	1.0
4	0.0	0.0	-	4	2.6	2.0	1.3	4	10.3	11.0	0.9
3	0.0	0.0	-	3	2.9	1.4	2.0	3	15.0	11.4	1.3
3	0.0	0.0	-	3	6.2	2.0	3.2	3	17.5	10.0	1.7
2	0.0	0.0	-	2	2.1	3.3	0.6	2	10.1	14.9	0.7
correlation coefficient			-	correlation coefficient			-0.500	correlation coefficient			0.020

B



C



D

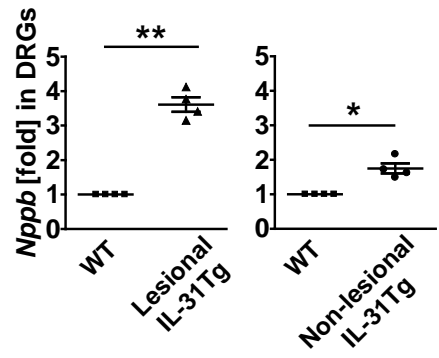


Fig. 4

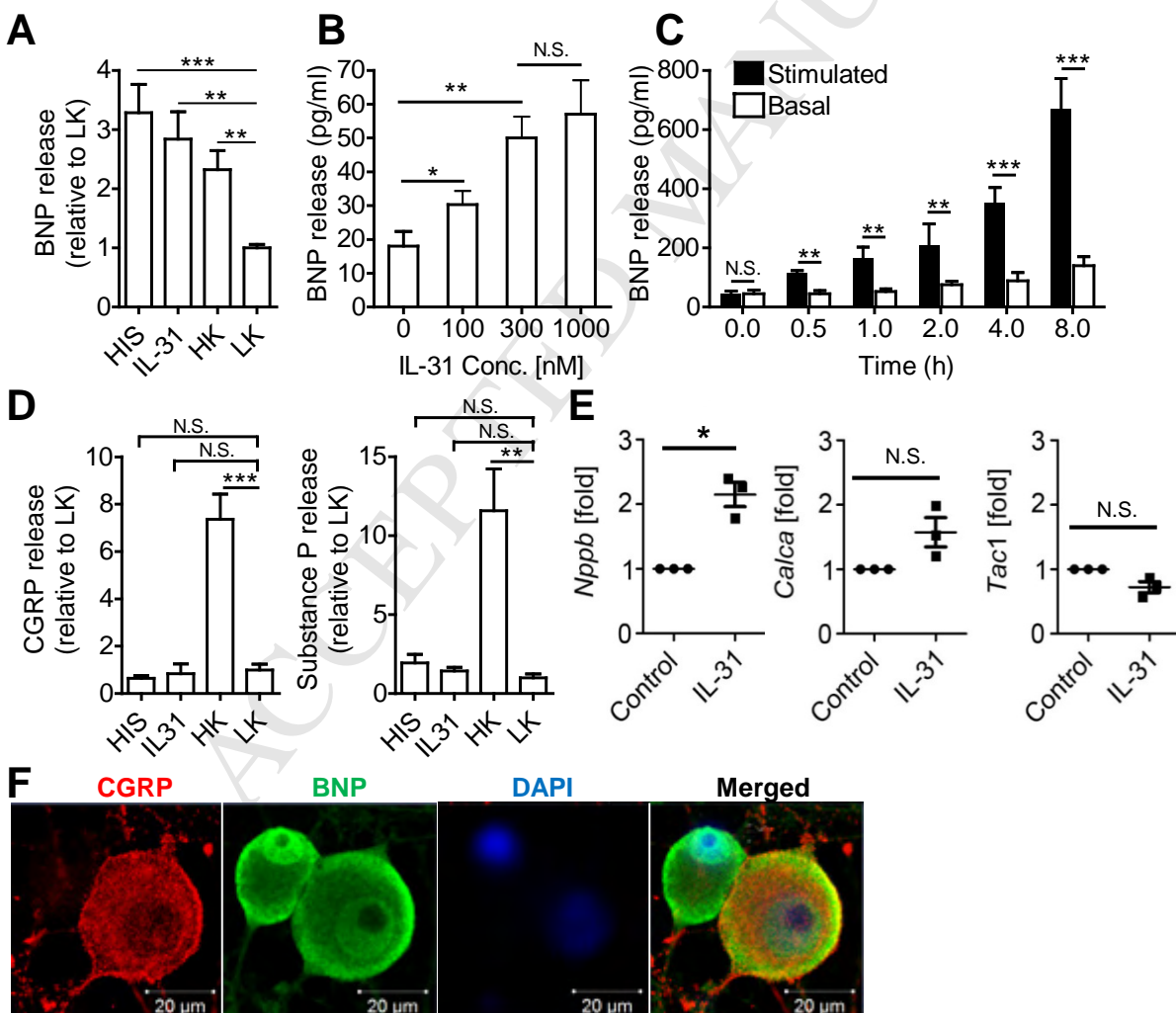


Fig. 5

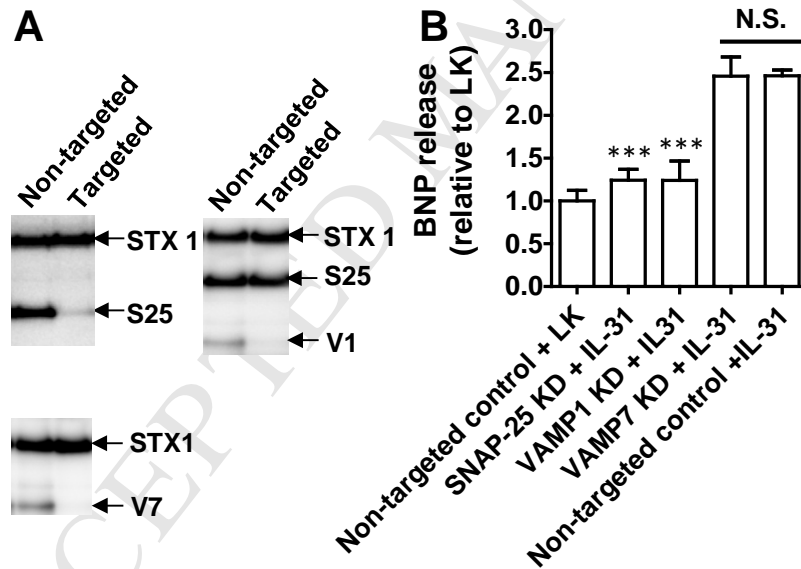


Fig. 6

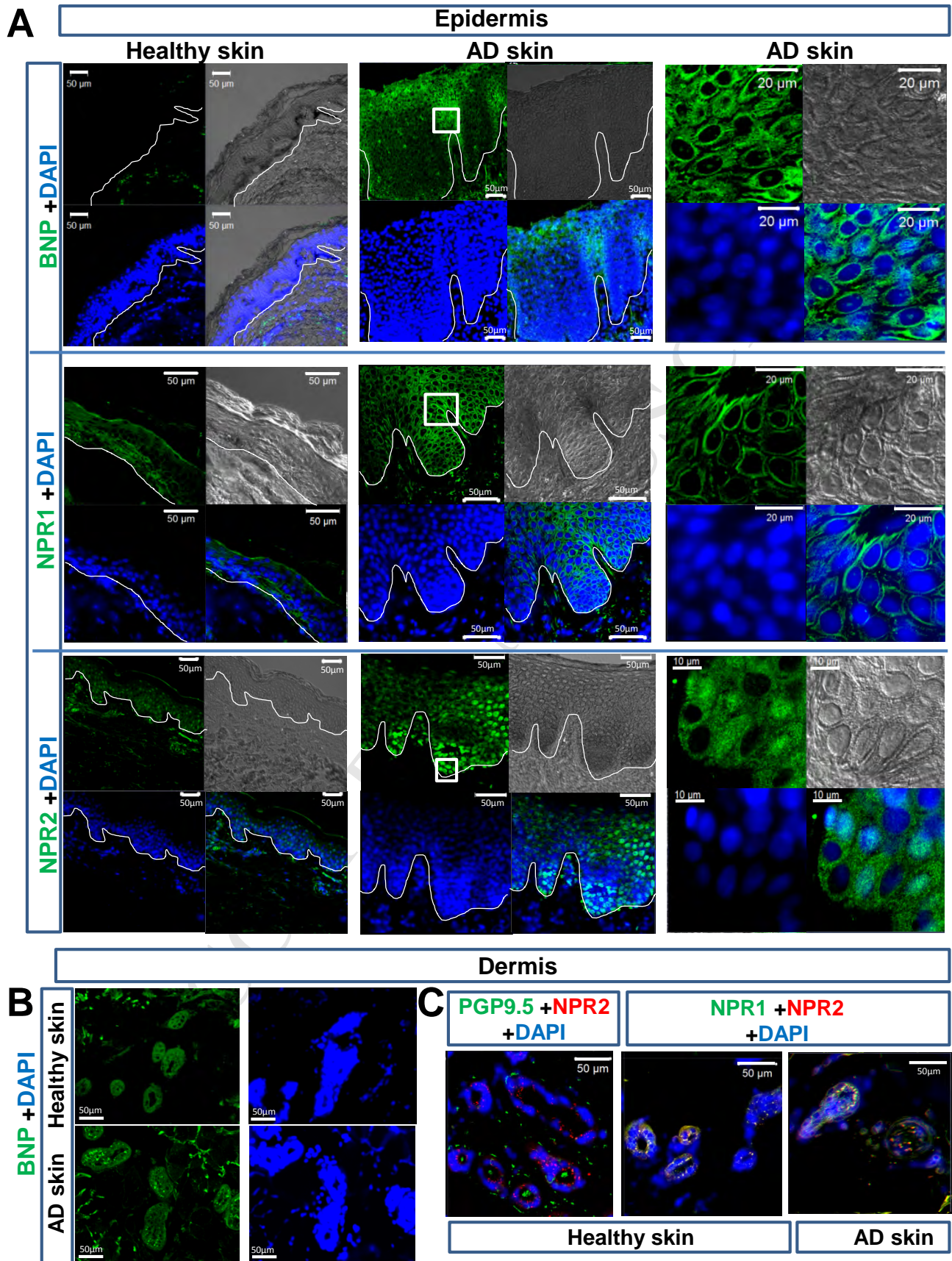


Fig. 7

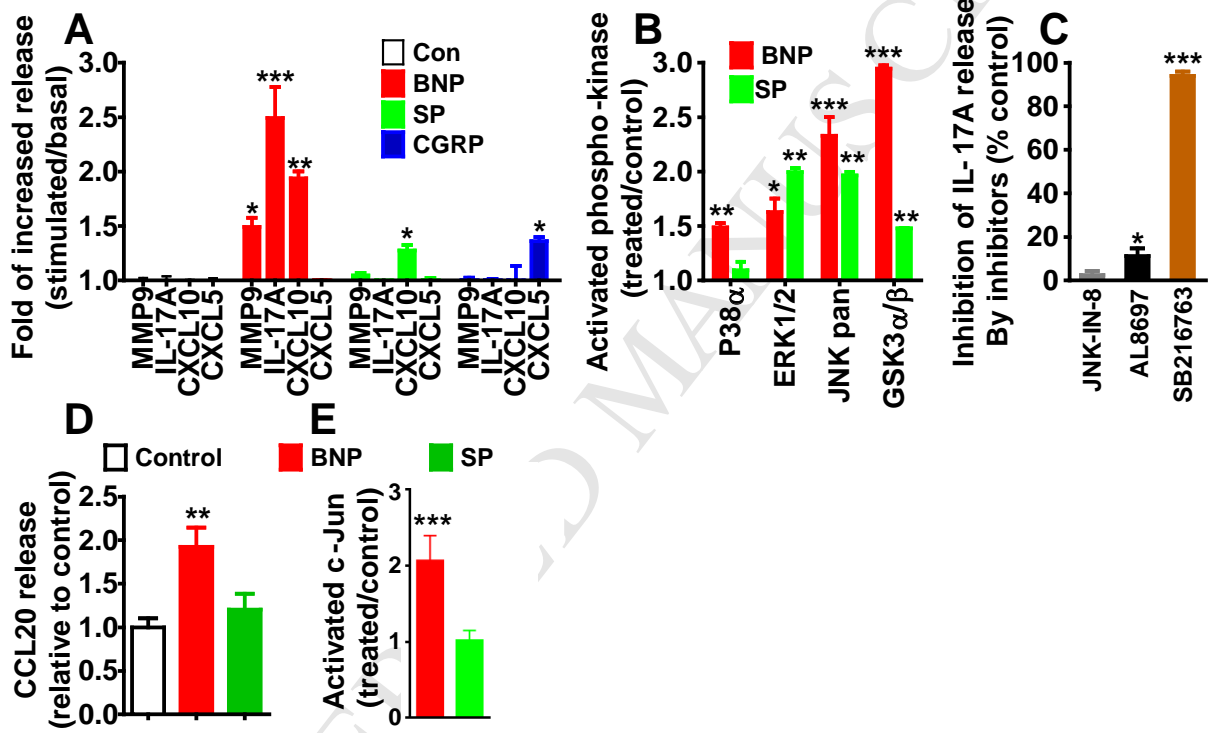
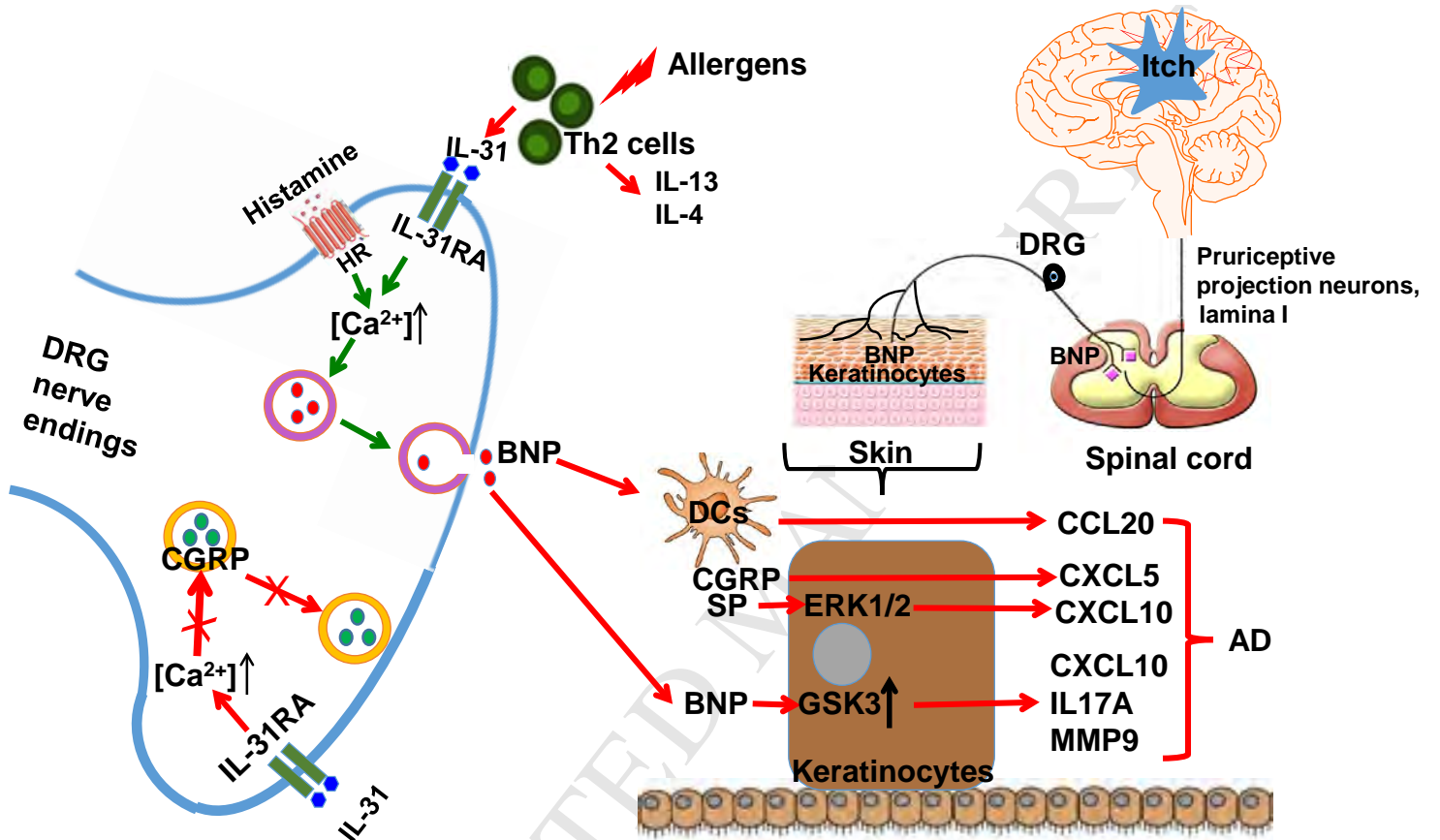


Fig. 8



Supplemental Materials and Methods

Materials

Skin samples from AD and healthy controls were bought from Tissue Solutions Ltd., Glasgow, Scotland. Enzyme immuno-assay (EIA) kits for CGRP and SP were bought from Bioquote; rabbit anti-syntaxin 1, rabbit anti-VAMP1 and 7 were bought from Synaptic Systems GmbH. SP, BNP, CGRP, histamine and ET-1, monoclonal antibody specific for CGRP (4901), rabbit anti-PGP9.5, ELISA kit for BNP, shRNA lentiviral particles were bought from Sigma-Aldrich. Donkey anti-rabbit Alexa-488 and anti-mouse Alexa-594, donkey anti-goat Alexa594 and anti-mouse Alexa 488 were supplied by Jackson ImmunoResearch. Ibidi GmbH provided the culture chambers. Rabbit anti-BNP antibody (G-011-23) was purchased from Phoenix Pharmaceuticals, Inc. and monoclonal anti-SNAP-25 (SMI 81) was bought from Sternberger Monoclonals Inc. Mouse monoclonal anti-PGP9.5 (Ab8189), -NPR2 (Ab55724), rabbit anti-NPR1 (Ab14356), -BNP (Ab19645), -NeuN antibody (Ab177487) and IL-17A ELISA kit were provided by Abcam; AL8697, goat anti-IL-31RA, mouse anti-OSMR β , CCL20 ELISA kit, proteome profilerTM human XL cytokine array, human phospho-kinase array kits and IL-17A antibody (AF-317-NA) were bought from R&D Systems; SB216763 was purchased from Tocris; JNK-IN-8 was obtained from Axon Medchem. Rabbit anti-NPR1 antibody (NBP1-31333) was purchased from Novus Bio. Adult normal hKCs and hDCs and their culture medium were bought from Lonza. Human DRG paraffin sections were bought from Zyagen. Alexa 594 conjugated mouse anti-human Vimentin antibody, Alexa 488 conjugated mouse anti-human CD4 and Alexa 488 conjugated mouse anti-human CD80 were purchased from BioLegend. Mouse C57 DRG sections were purchased from Amsbio.

HDM application on Grhl3PAR2^{+/+} mice model

The Grhl3PAR2^{+/+} mice were maintained in C57BL6/J-129X1/SvJ mixed strain and used for the experiments as AD model. We used mite-extract ointment/house dust mite (HDM) (BiostirAD cat#303-34131) on the right cheek to induce severe skin lesion. For HDM treatment, 8 mice were shaved on cheek one day prior to application. On the application day, 4% SDS was always rubbed on shaved cheek area 2 h before HDM application. HDM was applied on right cheek twice a week with at least a 3 day resting period prior to the next application for 6 weeks. At the

end of the treatments we euthanized the mice and harvest lesional, perilesional and non-lesional skin for pathologic diagnosis using HE staining to measure the clinical score, and trigeminal ganglia were harvested for gene expression experiment.

RNA-Seq

For gene expression experiment, TGs were harvested from *Grhl3PAR2*^{+/+} mice. Total RNA was isolated from right TG (ipsilateral) and left TG (contralateral) with TRIzol Reagent (Life technologies cat#15596). Then mRNA library was made with Ovation Universal RNA-Seq System (NuGEN cat#0343). Samples were subsequently sequenced on the HiSeq2500 (illumine).

Quantitative real time PCR

DRGs were isolated from adult C57Bl6 mice (6-8 weeks old) and treated with 3 mg/ml collagenase (Sigma Aldrich) and 0.25 mg/ml trypsin (PAA) for 30 minutes. DRGs were triturated for dissociation and were plated onto cell culture dishes coated with poly-L-lysine (100 mg/ml; Sigma Aldrich) and laminin (5 mg/ml; Sigma Aldrich) in MEM supplemented with 10% horse serum, 1% penicillin/streptomycin, 1% vitamins, 1% N2-supplement and 2% B27-supplement. After overnight rest, DRG neurons were treated with 100 ng/ml murine IL-31 (ZymoGenetics) for 6 h. The quantitation of mRNA levels was performed by real time fluorescence detection using Absolute SYBR Green ROX mix (ABI).

The primers used for both DRGs and skin were as follows: *mNppb* forward, 5'-gtcagtcggttgggctgtaac-3'; *mNppb* reverse, 5'-agaccagcagagtcagaa-3'; *mCalca* forward, 5'-agcaggaggaagagcagga-3'; *mCalca* reverse, 5'-cagattcccacaccgcttag-3'; *mTac1* forward, 5'-agcctcagcagttcttggga-3'; *mTac1* reverse, 5'-tctggccatgtccataaagag-3'. Primer and probe specific for 18S RNA and glyceraldehyde 3-phosphate dehydrogenase (GADPH) were obtained from Life technologies (Darmstadt, Germany) and Eurofins Genomics (Germany). Target gene expression was analyzed on an ABI Prism 7000 supplemented with SDS 1.2.3 software and the expression profile was normalized using the 18S or GADPH expression. In the case of mouse tissue, the primers used were: *mNPR1* forward, 5'-ttccactggaggttctggct-3'; *mNPR1* reverse, 5'-ctctgagaccagctcctttcc-3'.

BNP, CGRP and SP release assay

In order to investigate BNP, SP and CGRP release, DRG were isolated from postnatal d5 C57BL/6 mice and dissociated by collagenase I as detailed (1). Neurons were cultured in the presence of cytosine β -d-arabinofuranoside (AraC, Sigma) and nerve growth factor (NGF) 100 ng/ml for 7 DIV (days *in vitro*). Basal low potassium (LK) release buffer (mM; 22.5 HEPES, 135 NaCl, 3.5 KCl, 1 MgCl₂, 2.5 CaCl₂, 3.3 glucose and 0.1% BSA, pH 7.4) was added into each well, followed by a 30-min incubation at 37 °C (2). Cells were then stimulated for 30 min or as indicated in Figures by high potassium (HK, 60 mM K⁺, isotonicity balanced with NaCl), 1 μ M histamine, or 300 nM IL-31 (Zymogenetics). Release of BNP, CGRP or SP was quantified using their ELISA or EIA kit.

Measurement of intracellular Ca²⁺ concentration

For the hDRG calcium measurement, cells in culture were loaded with 5 μ M Fluo 8-AM (AAT Bioquest 21081) containing 0.1% Pluronic F-127 (Sigma P2443) for 20 min. Extracellular solution contained in mM: 145 NaCl, 3 KCl, 2 CaCl₂, 1 MgCl₂, 10 HEPES, 10 glucose adjusted to pH 7.4 with NaOH. Fluo-8-loaded cells were excited at 480 nm and emission was collected at 520 nm with a pcoEDGE sCMOS camera (PCO) mounted on an inverted microscope (Olympus IX71). Following a baseline period of 60 s, ET-1 (30 nM); Histamine (10 μ M); IL-31 (300 nM) were applied sequentially, for 60 s. each, followed by washout for 5 min. Images were acquired at 0.2 Hz. In the case of mDRGs, 3 μ M Fluo 4-AM was used and images were acquired by a Zeiss LSM710 confocal microscope (Carl Zeiss MicroImaging) with argon laser at 2 sec intervals.

Immunofluorescence staining

For cellular localization of CGRP and BNP in cultured mDRGs, cells were processed by dual labelling overnight at 4°C with 1:100 rabbit anti-BNP antibody (G-011-23; Phoenix Pharmaceuticals, Inc.) and 1:200 mouse anti-CGRP antibody (clone 4901, Sigma). Secondary donkey anti-rabbit Alexa Fluor 488 (1:2000) and anti-mouse Alexa Fluor 594 (1:2000) were added for 1 h at room temperature.

Human DRG and skin paraffin sections (15 μ m) were deparaffinized, rehydrated before permeabilized in phosphate-buffered saline with 0.2% Triton X-100 (PBS-T) and then incubated

in PBS containing 5% normal donkey serum (blocking solution) at RT for 1 h. Specimens were then incubated with primary antibodies in blocking solution (4 °C, overnight). For human DRG sections, primary antibodies were used at the following dilutions: goat anti-IL-31RA 1:100 (R&D Systems); mouse anti-OSMR β 1:100 (R&D Systems); mouse monoclonal PGP9.5 antibody 1:40 (Abcam) or rabbit anti-PGP9.5 1:1000 (Sigma); rabbit anti-NeuN antibody 1:500 (Abcam). The sections were washed in PBS and were incubated in donkey anti-goat Alexa 594 and donkey anti-mouse Alexa 488 (Jackson ImmunoResearch) or donkey anti-rabbit Alexa 488 diluted 1:2000 with blocking solution (RT, 1 h). For human skin sections (15 μ m), we used rabbit polyclonal to BNP (Abcam, 1:1000), rabbit polyclonal to NPR1 (Novus Bio, 1:500) or mouse monoclonal to NPR2 (Abcam, 1:80), rabbit anti-PGP9.5 (Sigma).

For hKC staining, cultured cells were fixed in 3.7% paraformaldehyde in PBS, permeabilized by 0.1% Triton X-100 and then blocked in 5% normal donkey serum (blocking solution) at RT for 1 h before samples were incubated with the primary antibodies overnight at 4 °C. Antibodies used are: rabbit anti-NPR1 1:500 (Abcam), rabbit anti-BNP 1:1000 (Abcam), mouse monoclonal to NPR2 1:80 (Abcam), mouse monoclonal to K14 1:200 (cytokeratin 14; Ab7800), goat anti-IL-17A 1:100 (R&D), Alexa 594 conjugated mouse anti-human Vimentin antibody 1:200, Alexa 488 conjugated mouse anti-human CD4 1:200 and Alexa 488 conjugated mouse anti-human CD80 1:200. The specimens were washed in PBS and were incubated in donkey anti-goat Alexa594 or donkey anti-goat 488 and donkey anti-mouse Alexa 488 or donkey anti-rabbit Alexa 488 (Jackson ImmunoResearch) diluted 1:2000 with blocking solution (RT, 1 h).

To check specificity of BNP and CGRP antibodies, rabbit anti-BNP antibody (G-011-23; Phoenix Pharmaceuticals, Inc.) was pre-incubated with or without mouse BNP-45 peptide (Phoenix Europe) at 1:10 molar ratio. Likewise, mouse anti-CGRP antibody (clone 4901, Sigma) was pre-incubated with or without rat α -CGRP peptide (Sigma) at 1:10 molar ratio. Antibodies alone or with their antigen mixtures were incubated at overnight at 4°C. Mouse C57 DRG sections purchased from Amsbio were formalin-fixed, permeabilised in PBS with 0.1% Triton X-100 and blocked in PBS containing 5% normal donkey serum. Immunofluorescence labelling was performed overnight at 4°C with 1:100 rabbit anti-BNP antibody, 1:200 mouse anti-CGRP antibody alone or antibody pre-incubated with its antigen (as specified in figure legends) in blocking solution. After extensive wash, secondary donkey anti-rabbit Alexa Fluor 488 (1:2000)

and anti-mouse Alexa Fluor 594 (1:2000) diluted in blocking solution were added for 1 h at room temperature.

After the final wash of the secondary antibody, specimens were mounted onto slides using prolong anti-fade reagents contain (4',6-diamidino-2-phenylindole) DAPI (ThermoFisher Scientific). Images were taken by a Zeiss LSM710 confocal microscope (Carl Zeiss MicroImaging) with argon and helium/neon lasers. Images were acquired by Zen software (Universal Imaging, Göttingen).

Lentivirus-mediated knockdown of SNARE proteins

At 7 DIV, mDRGs were incubated in medium containing shRNA lentiviral particles that specifically target to SNAP-25, VAMP1, or VAMP7, or non-targeted PLK0.1-puro particles (400 transducing units/well), and cultured as above. After 7–10 days in culture, cells were stimulated before being harvested in lithium dodecyl sulfate sample buffer and analysed by western blotting. Targeted genes/protein IDs and validated sequences for shRNA lentiviral transduction particles were as follows:

NM_011428,SNAP-25:

CCGGCATCAGGACTTTGGTTATGTTCTCGAGAACATAACCAAAGTCCTGATGTTTTT
G

NM_009496,VAMP1:

GTACCGGCATCGTGGTAGTGATTGTAATCTCGAGATTACAATCACTACCACGATGTT
TTTTG;

NM_011515,VAMP7:

CCGGGCACAAGTGGATGAACTGAACTCGAGTTTCAGTTCATCCACTTGTGCTTTTT
G

Culture of human primary epidermal keratinocytes (hKCs) and human monocyte-derived dendritic cells (hDCs), cytokine antibody array and phosphor-kinase array

Human primary KCs were cultured in the KBM-Gold™ medium with KBM-Gold SingleQuot keratinocytes supplement (Lonza). All the release from hKCs was performed in hydrocortisone-free medium with or without stimulation compound. Human DCs were cultured by *in vitro*

differentiation of CD14⁺ monocytes (subpopulation of peripheral blood mononuclear cells) using LGM-3TM Lymphocyte Growth Medium + 50 ng/ml GM-CSF + 50 ng/ml IL-4 (Lonza). Cells were maintained in the above medium for 3 d before use. Release was performed in plain LGM-3TM Lymphocyte Growth Medium in the presence of neuropeptides. After release, cell culture supernatant was collected for proteome profiler human cytokine antibody array according manufacturer protocol. Briefly, the array membranes were blocked and then incubated with the sample for overnight at 4 °C. The membranes were washed three times and then incubated in diluted primary antibodies for 1 h at room temperature. After washing, membranes were incubated with diluted HRP-conjugated streptavidin for 1 h at room temperature and membranes were developed using enhanced chemiluminescence reagent. Images were captured, densitometrically scanned. Each cytokine spot was analyzed using Image J software and the average of positive controls of each treatment was set to 100 and all cytokines of the treatment were compared to that. The resultant values from the treatment were calculated relative to the non-treated control to give the fold of increase.

For the kinase array, cells grown in T175 flasks were treated with or without neuropeptides for 8 min and cells were lysed for intracellular phosphor-kinase array according to manufacturer protocol.

Phospho-kinase inhibitors treatment

1 μ M selective p38 MAPK inhibitor AL8697, 1 μ M selective inhibitor of the α and β isozymes of GSK-3 SB216763 or 1 μ M selective JNK1/2/3 inhibitor JNK-IN-8 was applied to the cultured hKCs 1 h prior to and during 24 h incubation with 1 μ M BNP or 1 μ M SP in serum free and hydrocortisone-free medium to release the cytokines. The supernatant was collected for assay of cytokines using antibody array or ELISA as detailed above.

Reference for Supplementary Methods

1. Malin SA, Davis BM, and Molliver DC. Production of dissociated sensory neuron cultures and considerations for their use in studying neuronal function and plasticity. *Nature protocols*. 2007;2(1):152-60.
2. Meng J, Ovsepian SV, Wang J, Pickering M, Sasse A, Aoki KR, Lawrence GW, and Dolly JO. Activation of TRPV1 mediates calcitonin gene-related peptide release, which excites trigeminal

sensory neurons and is attenuated by a retargeted botulinum toxin with anti-nociceptive potential. *The Journal of neuroscience : the official journal of the Society for Neuroscience*. 2009;29(15):4981-92.

ACCEPTED MANUSCRIPT

Supplementary Figure Legends

Fig E1. Average *Nppb* value FPKM from contralateral cheeks of top 3 clinical scored *Grhl3PAR2*^{+/+} mice was not significantly different from that of the WT mice.

Statistical analysis demonstrated that *Nppb* FPKM from the non-treated contralateral cheeks of *Grhl3PAR2*^{+/+} mice did not significantly differ from the values of Vaseline-treated ipsilateral cheeks or non-treated contralateral cheeks in WT mice. However, HDM induced significantly higher *Nppb* FPKM in ipsilateral cheeks compared with contralateral cheeks in *Grhl3PAR2*^{+/+} mice. Average values of FPKM are plotted. $P < 0.05$ indicates significance.

Fig E2. IL-31-induced *Nppb* mRNA synthesis in cultured mouse DRGs is time- and concentration dependent.

A, RT-PCR analysis of *Nppb* mRNA synthesis in mDRGs upon treatment with various concentrations of IL-31 for 30 min. **B**, Time course of *Nppb* mRNA synthesis analysed by RT-PCR after treatment with 300 nM IL-31. Data are expressed relative to GAPDH and presented as mean \pm S.E.M. $n = 3$ independent experiments. N.S. > 0.05 ; ** $P < 0.01$; *** $P < 0.001$.

Fig E3. Antibody absorption test confirmed BNP and CGRP antibodies' specificities. A, Confocal images show that fluorescence signal of CGRP in mDRG sections was greatly reduced by pre-absorption of CGRP antibody with α -CGRP peptide. **B**, Immunofluorescence images showing staining pattern in mDRG sections using BNP antibody in comparison with its antigen absorbed control.

Fig E4. Characterization of cultured human primary keratinocytes (hKCs) using immunocytochemical staining.

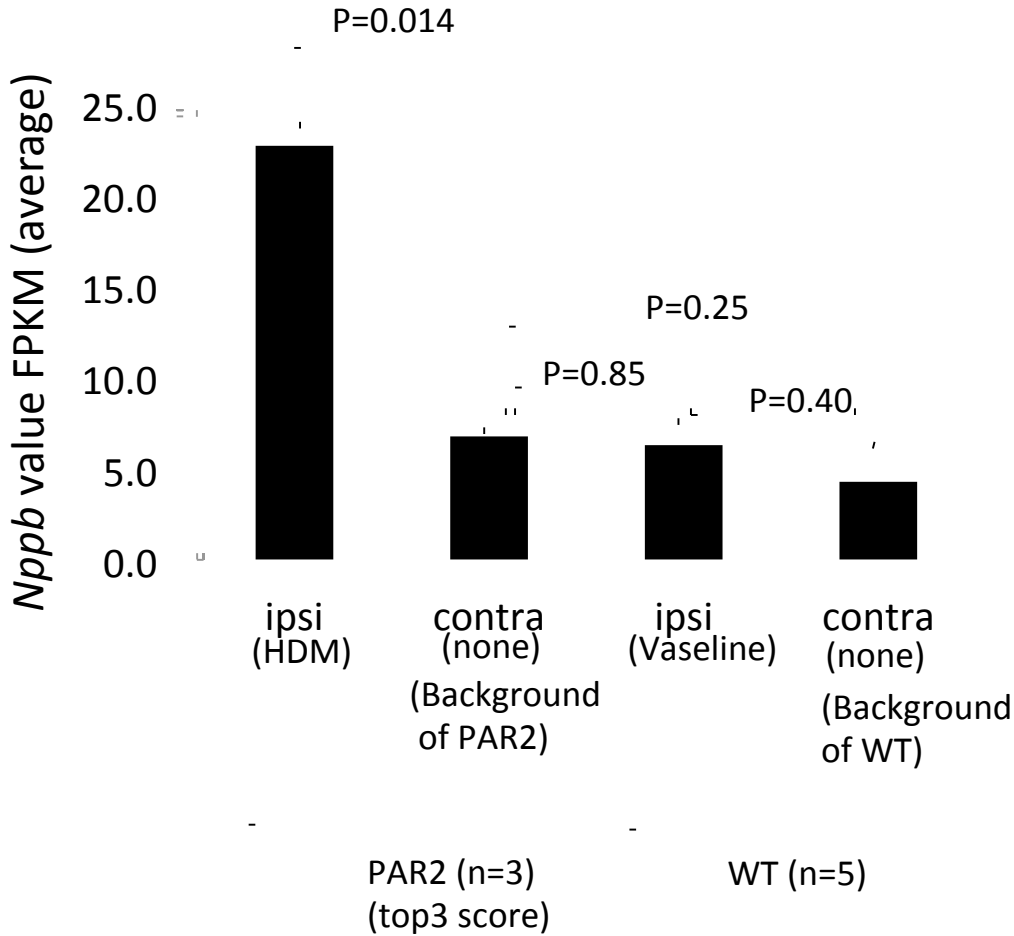
A, Immunofluorescence staining of BNP, NPR1 and NPR2 as well as proliferative keratinocyte marker Keratin 14 (K14) in hKCs. BNP was undetectable. NPR1 and NPR2 showed distinct distribution pattern. **B**, IL-17A immune-signal is detected in cultured hKCs. K14 and vimentin were expressed in all the cultured cells. Immuno-cell markers, CD4 and CD80 antibody staining signal is either absent or negligible.

Fig E5. Immunohistochemical dual staining of NPR1 and NPR2 in skin of human healthy control and patient with AD. Representative fluorescent images at low magnification (left column panels) and high magnification (right column panels) of NPR1 and NPR2 in healthy control (**A**) and AD patient skin (**B**). NPR1 and 2 are highly localized in some cells in the dermis. Specimens were counter-stained with DAPI.

Fig E6. RT-PCR analysis of *Nppb* and NPR1 mRNA levels in skin of IL-31Tg or WT mice.

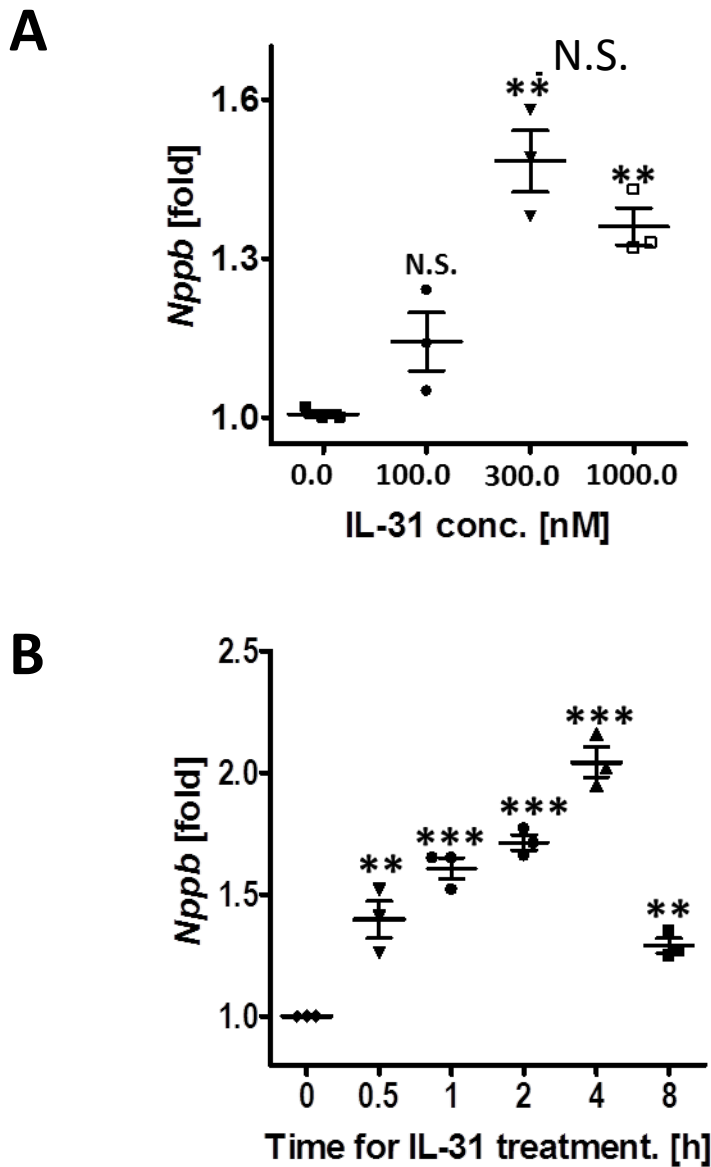
RT-PCR analysis of *Nppb* mRNA (**A**) or NPR1 mRNA (**B**) levels in skin isolated from lesional, nonlesional IL-31Tg or WT mice. Values were normalized to the housekeeping gene GAPDH. The results (mean \pm S.E.M.) are pooled data from multiple animals. Significant difference is indicated; N.S. $P > 0.05$; * $P < 0.05$; ** $P < 0.01$, *** $P < 0.001$.

Fig E1



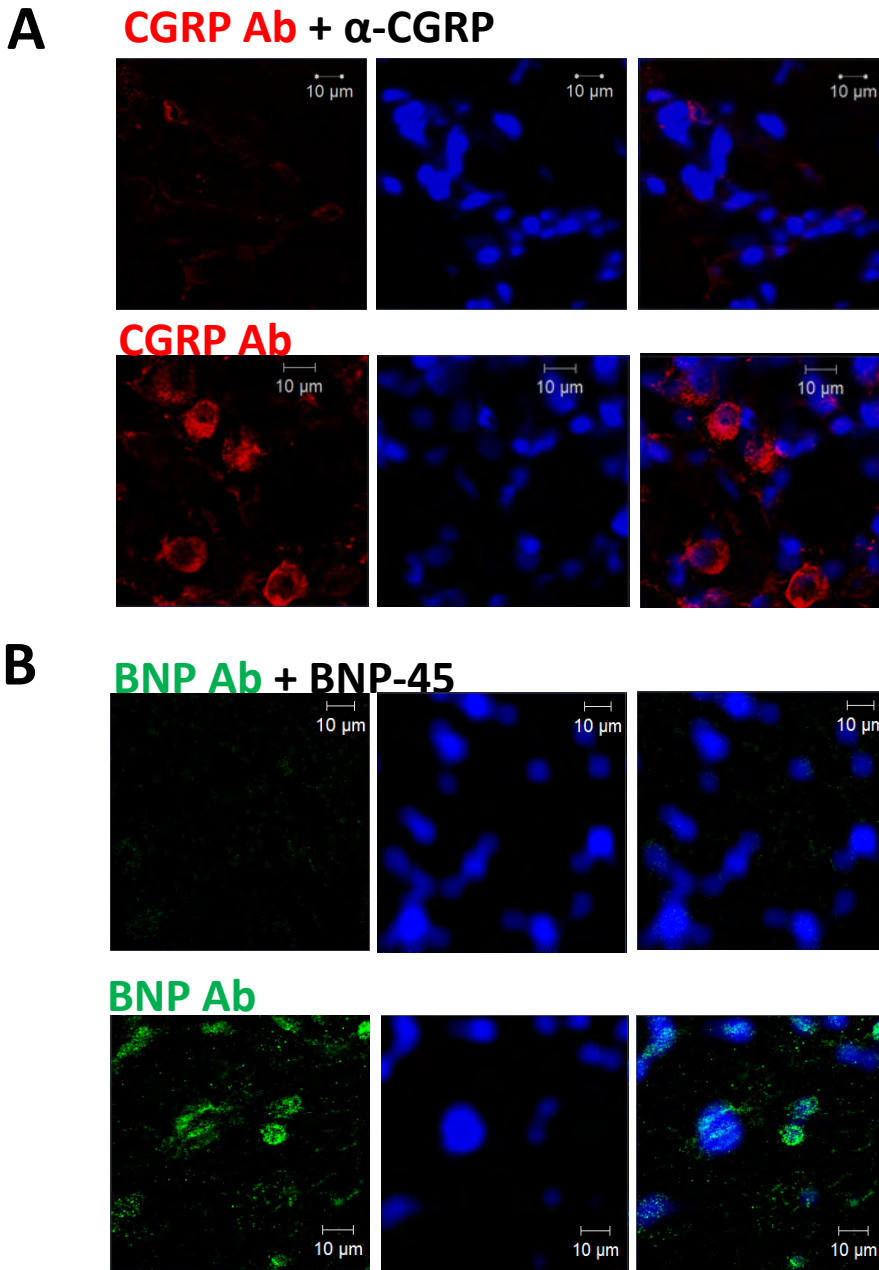
Average *Nppb* value FPKM from contralateral cheeks of top 3 clinical scored *Grhl3*PAR2^{+/+} mice was not significantly different from that of the WT mice. Statistical analysis demonstrated that *Nppb* FPKM from the non-treated contralateral cheeks of *Grhl3*PAR2^{+/+} mice did not significantly differ from the values of Vaseline-treated ipsilateral cheeks or non-treated contralateral cheeks in WT mice. However, HDM induced significantly higher *Nppb* FPKM in ipsilateral cheeks compared with contralateral cheeks in *Grhl3*PAR2^{+/+} mice. Average values of FPKM are plotted. P < 0.05 indicates significance.

Fig E2



IL-31-induced *Nppb* mRNA synthesis in cultured mouse DRGs is time- and concentration-dependent. **A**, RT-PCR analysis of *Nppb* mRNA synthesis in mDRGs upon treatment with various concentrations of IL-31 for 30 min. **B**, Time course of *Nppb* mRNA synthesis analysed by RT-PCR after treatment with 300 nM IL-31. Data are expressed relative to GAPDH and presented as mean \pm S.E.M. n = 3 independent experiments. N.S. P>0.05; ** P<0.01; *** P<0.001.

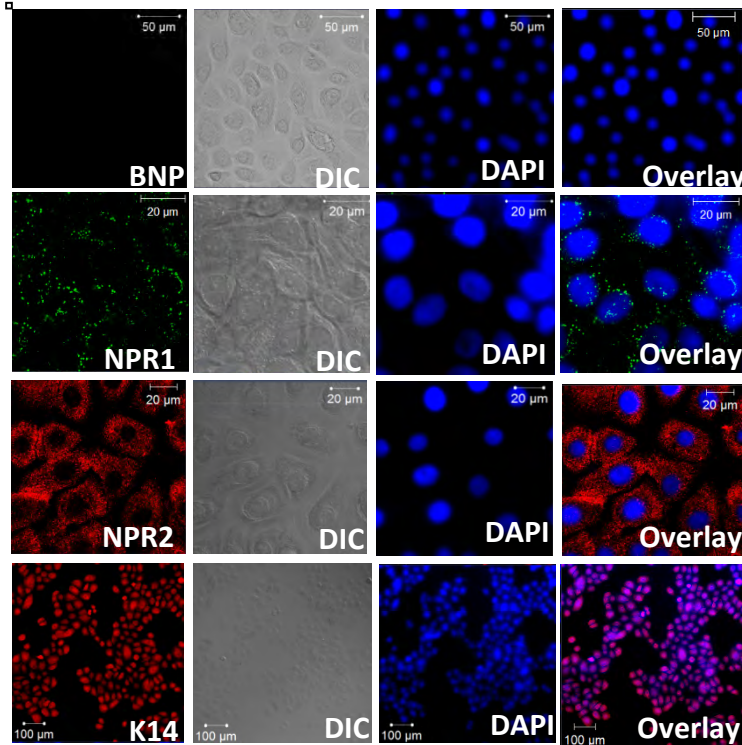
Fig E3



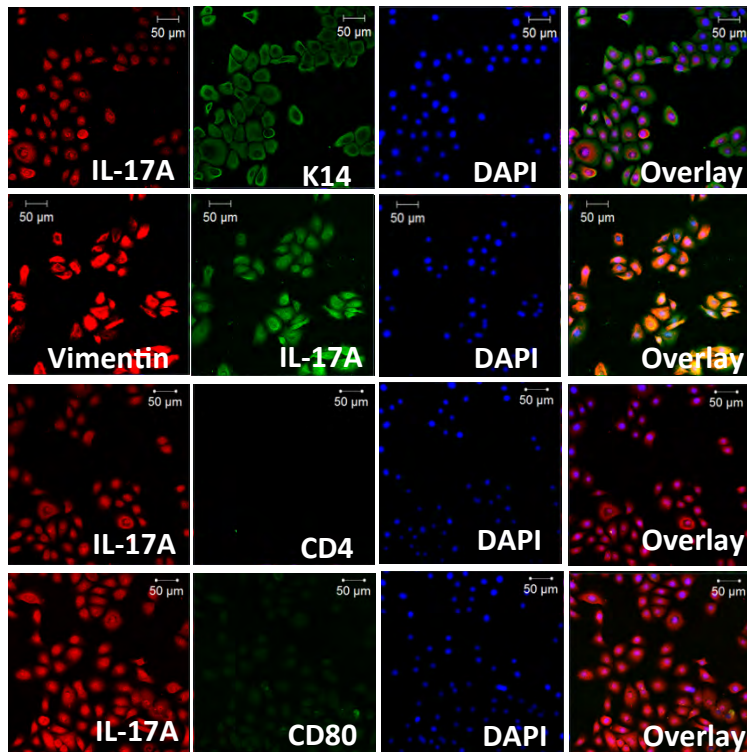
Antibody absorption test confirmed BNP and CGRP antibodies' specificities. A, Confocal images show that fluorescence signal of CGRP in mDRG sections was greatly reduced by pre-absorption of CGRP antibody with α -CGRP peptide. **B,** Immunofluorescence images showing staining pattern in mDRG sections using BNP antibody in comparison with its antigen absorbed control.

Fig E4

A

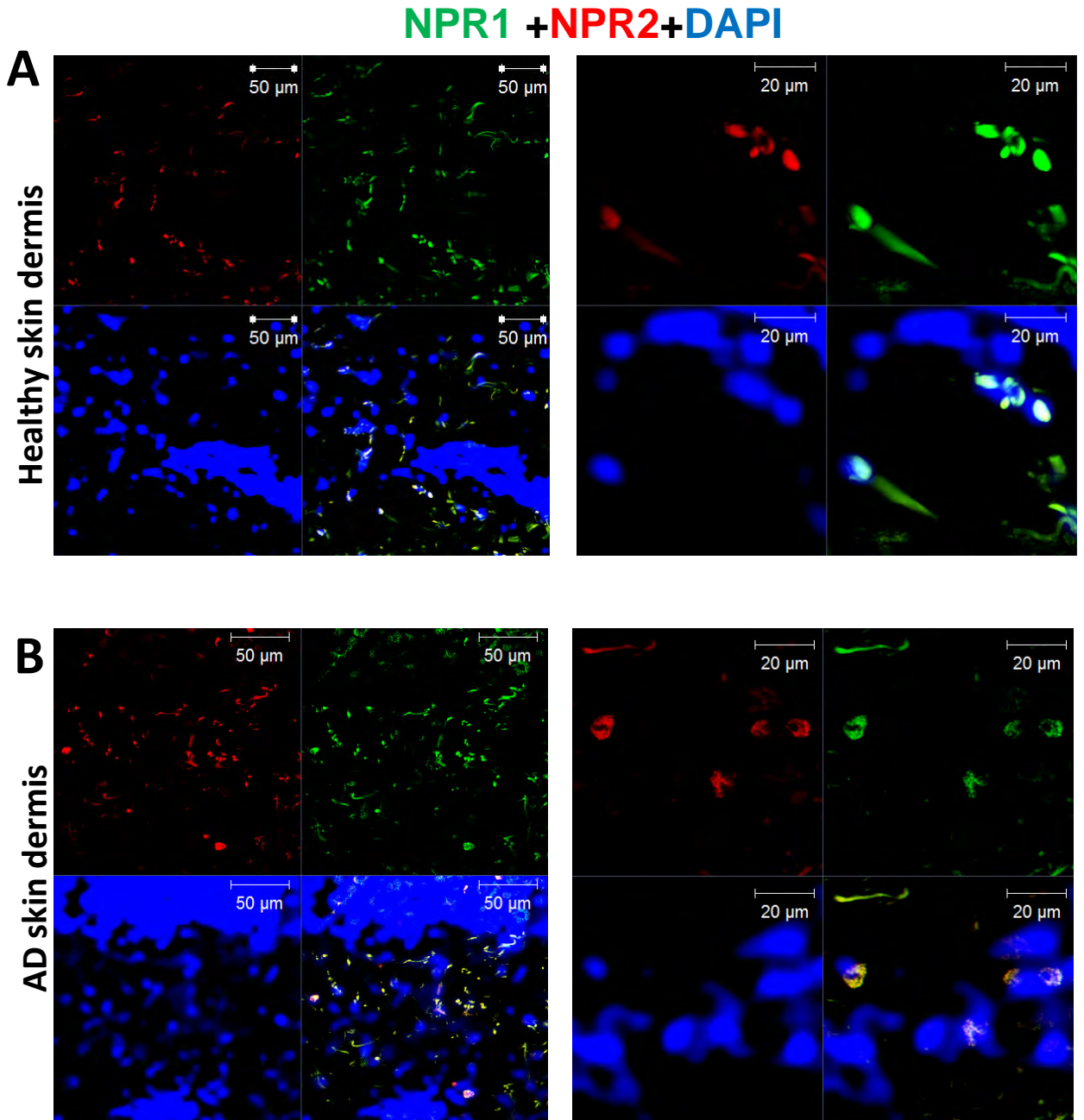


B



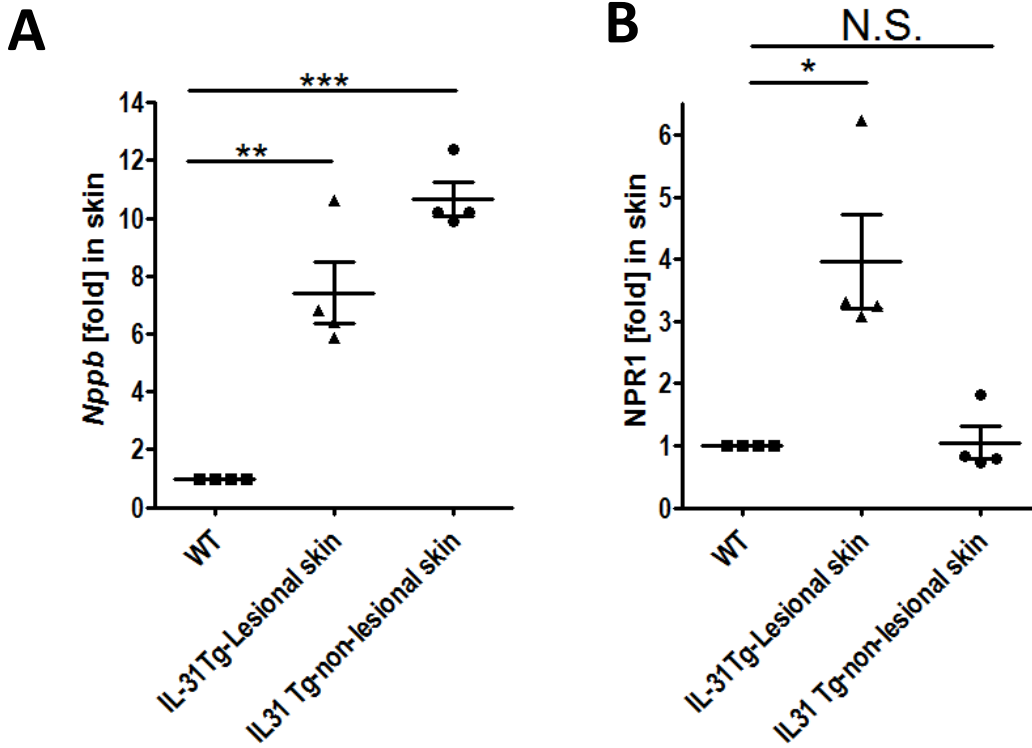
Characterization of cultured human primary keratinocytes (hKCs) using immunocytochemical staining. **A**, Immunofluorescence staining of BNP, NPR1 and NPR2 as well as proliferative keratinocyte marker Keratin 14 (K14) in hKCs. BNP was undetectable. NPR1 and NPR2 showed distinct distribution pattern. **B**, IL-17A immune-signal is detected in cultured hKCs. K14 and vimentin were expressed in all the cultured cells. Immuno-cell markers, CD4 and CD80 antibody staining signal is either absent or negligible.

Fig E5



Immunohistochemical dual staining of NPR1 and NPR2 in skin of human healthy control and patient with AD. Representative fluorescent images at low magnification (left column panels) and high magnification (right column panels) of NPR1 and NPR2 in healthy control (A) and AD patient skin (B). NPR1 and 2 are highly localized in some cells in the dermis. Specimens were counter-stained with DAPI.

Fig E6



RT-PCR analysis of *Nppb* and NPR1 mRNA levels in skin of IL-31Tg or WT mice. RT-PCR analysis of *Nppb* mRNA (A) or NPR1 mRNA (B) levels in skin isolated from lesional, non-lesional IL-31Tg or WT mice. Values were normalized to the housekeeping gene GADPH. The results (mean \pm S.E.M.) are pooled data from multiple animals. Significant difference is indicated; N.S. $P > 0.05$; * $P < 0.05$; ** $P < 0.01$, *** $P < 0.001$.